Delivery Reliability for Natural Gas -- Inspection Technologies

Phase I Topical Report

Reporting Period Start Date: September 30, 2004
Reporting Period End Date: September 30, 2005

GTI Project Manager: Albert Teitsma
GTI Principal Investigator: Julie Maupin

October 2005

DE-FC26-04NT42266

Prepared by:
Gas Technology Institute
1700 S. Mount Prospect Road
Des Plaines, Illinois 60018

DISCLAIMER

ABSTRACT

The Remote Field Eddy Current (RFEC) technique is ideal for inspecting unpiggable pipelines because all of its components can be made smaller than the diameter of the pipe to be inspected. For these reasons, RFEC was selected as a technology to be integrated with the Explorer II robotic platform for unpiggable pipeline inspections. The research work is a continuation of a prior DOE-NETL project but is now directed towards a seamless integration with the robot. The laboratory set-up has been improved and data collection is nearly autonomous. With the improved collections speeds, GTI has been able to test more variables. Tests have been run on 6” and 12” seamless and seam-welded pipes. Testing on the 6” pipes have included using five exciter coils, each of a different geometry. Two types of sensor coils have been tested. With a focus on preparing the technology for use on the Explorer II, improvements in power consumption have proved successful. Tests with metal components have been performed to check for interference with the electromagnetic field. The results of these tests indicate RFEC will produce quality inspections while on the robot. GTI has also been testing manufactured detection boards currently used for boiler tube inspections. These boards are appropriately compact for use on the Explorer II robot and are able to detect defects at the speed of robot travel. In addition to advanced sensor development, GTI has participated in sensor/platform definition and module design activities. Mechanical constraints, power requirements, limited control and communication protocols, and potential busses and connectors have been addressed. GTI has conducted a proper design process to produce a sound design for the RFEC components to fit into two modules. The remaining work to be performed in the design of the sensor module is packaging and strengthening.

TABLE OF CONTENTS

EXECUTIVE SUMMARY

The Remote Field Eddy Current (RFEC) Project (DE-FC26_04NT42266) supports the DOE-NETL Delivery Reliability for Natural Gas - Inspection Technologies program. This program seeks to enhance the integrity and reliability of the natural gas distribution and transmission systems across the United States to ensure the availability of clean, affordable energy for our homes, businesses and industries by developing technologies that improve the safety and delivery reliability of the natural gas infrastructure. This project is aimed at increasing safety and reducing unplanned operational outages by developing an inspection tool for "unpiggable" pipelines, which cannot be inspected with available technologies due to various restrictions in the pipeline. The inspection tool is envisaged as a combination of the Explorer II robot and a sensor technology. This project focuses on the Remote Field Eddy Current technology as the sensing technology and its development for integration with the robot. There are three phases, Design, Construction, and Integration and Demonstration, where the last phase integrates the RFEC inspection technology with the robot and proves the combined system's efficacy in an operating pipeline. Currently, the project is at the end of the Design phase, Phase I.

The RFEC technology is well suited for unpiggable pipelines because its components can be made much smaller than the pipe diameter it is inspecting. The components can be easily adapted to inspect pipelines with multiple diameters, valve and bore restrictions, and tight bends. We are currently working on the mechanics, electronics, and sensor design to prepare RFEC for integration with the Explorer II robot.

We have completed all of our deliverables, including the Research Management Plan, Technology Assessment Report, and Initial Sensor/Platform Definition. We attended the Kickoff Meeting held at Carnegie Mellon University's National Robotics Engineering Consortium. We also participated in multiple teleconferences to coordinate with other members of the program.

The laboratory is set up with seam welded and seamless pipes of 6" and 12" diameters. Each pipe has a set of 13 machined defects for testing and optimizing the technology for the robotic prototype. We have made significant improvements to the laboratory setup. At the start of the project, we could only test using one sensor coil. We built a multiplexer that can collect data from up to 16 sensor coils. We built a new test vehicle to mount multiple coils to and built an automatic winch system to pull the vehicle through the pipe in ¼" steps. We wrote LabVIEW programs to control the winch system and collect data from all the sensor coils. We can now inspect an entire pipe without an operator present in less time than it used to take us to scan a single defect. Additionally, we've obtained a Ferroscope from Russell Technologies that is capable of collecting data at the rate of travel achievable by the Explorer II robot. As a result, testing is much more efficient and allows us to test more variables in less time.

Some of the variables we have tested include exciter coil geometries. We tested five different exciter coils and two types of sensor coils. The optimal sensor coil is 20,000 turns of #46 copper wire wound on a 3/8" wide, ¾" diameter bobbin. The best results were achieved with an exciter coil of 900 turns of #28 copper wire wound 2.5" long on a 3.5" diameter spool. We were able to consistently detect defects as small as ½" diameter and 10% missing wall thickness. Because we can detect defects so much smaller than those that need to be detected in an operating pipeline, it is extremely unlikely that the RFEC technology would not detect a defect in the field that would require repairs. In addition, we have wound exciter coils that consumed less than1.85 Watts. Earlier coils consumed as much as 10 Watts. We have made limiting power consumption an important criteria for exciter coils. This is significant because Explorer II is an untethered system with a limited power supply.

Module design has been very promising. Early designs required three robot modules, one for

the exciter coil and two for sensor coils, to obtain 360° wall coverage. Through redesign, we developed three new module designs that were capable of housing all the sensor coils into one module, thereby eliminating the need for three modules. Through process of elimination, we chose the best design to move forward into the prototyping stage. At the present time, we are improving this design by making it stronger and working on the packaging aspects of the electronics. We are confident that this design is suitable for RFEC detection on Explorer II. With continued success, the natural gas industry will realize an innovative and powerful inspection tool created from the combination of RFEC technology and Explorer II.

THE REMOTE FIELD EDDY CURRENT TECHNIQUE

The remote field eddy current (RFEC) technique was patented by W. R. McLean (US Patent 2,573,799, “Apparatus for Magnetically Measuring Thickness of Ferrous Pipe”, Nov.6, 1951) and first developed by Tom Schmidt at Shell for down hole inspection (Schmidt, T. R., “The Casing Instrument Tool- …”, Corrosion, pp 81-85, July 1961). The RFEC technology has many advantages including:

- A simple exciter coil that can be less than 50% the diameter of the pipe. The exciter coil does not need to be close to the wall.
- Simple and small (millimeter to centimeter diameter) sensor coils that do not need to contact the wall. Thus, the diameter of the coil array can be easily adjusted to match the pipe diameter yet pass through a small opening.
- Sensor coils close to the pipe wall provide sensitivity and accuracy comparable to standard MFL inspection tools. General pipe corrosion of 10% of the wall thickness or less is detected and measured with commercial units.
- Sensor lift-off, up to 0.75 inch can be automatically compensated for, though sensitivity and resolution will be compromised.

The technique is commercially viable for inspecting boiler tubes and pipe diameters up to 8 inches for several hundred feet. Recently, Russell Technologies developed an 18 inch device that can inspect production wells for several thousand feet. However, none of the current versions are collapsible to 50% of the pipe diameter or less, nor can any handle short-radius elbows and other obstacles. To adapt the technique for this application will require investigating variations such as transmitter coil angle and methods for either reducing the variations or sensitivity to them. Larger diameters should not be a problem since specialized tools can inspect the steel reinforcing of 12 foot diameter concrete water mains (Atherton, D. L., US patent 6,127,823, “Electromagnetic Method for Non-Destructive Testing of Prestressed Concrete Pipes for Broken Prestressed Wires”, Oct. 3, 2000).

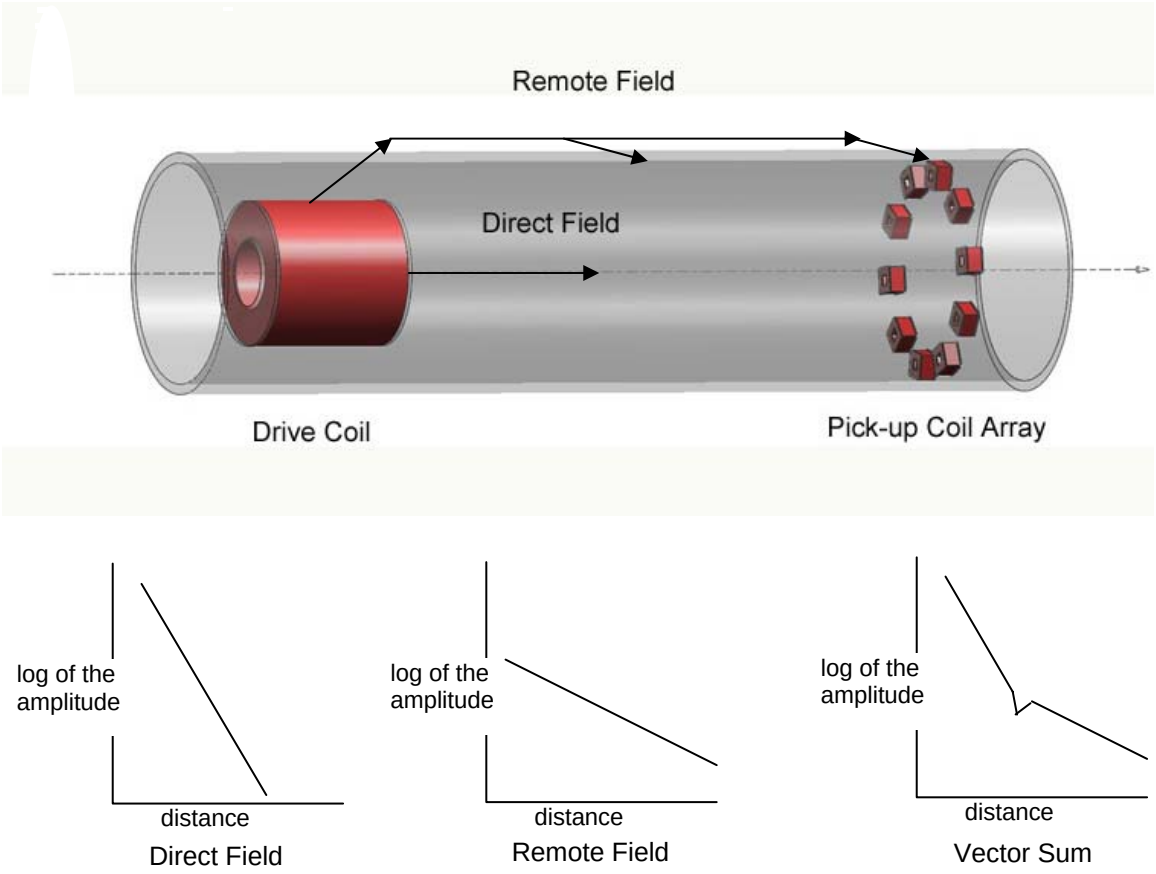

Figure 1: Variation of the amplitude of propagating fields with distance along a pipe. The sum includes the effect of the phase difference between the direct and remote field vectors. In the presence of metal loss, the signal amplitude increases while the phase change decreases. Measurements far from the exciter coil are very sensitive to corrosion and insensitive to the direct field.

Figure 1 shows the basics of the remote field eddy current (RFEC) method. The exciter coils sends 20 Hz to 200 Hz electromagnetic waves propagating down the pipe and through the pipe wall. The electromagnetic waves traveling inside the pipe (direct field) are highly attenuated because they are well below the cutoff frequency for propagation in a wave-guide. As far as the electromagnetic waves are concerned, a pipeline is nothing more than a wave-guide. Approximately two pipe diameters from the source coil, these waves all but vanish. Meanwhile, the waves that have penetrated the wall (remote field) can penetrate back into the pipe as well. At about two pipe diameters from the exciter coil and beyond, these waves swamp the direct field waves attempting to propagate down the bore of the pipe and, therefore, can be detected and measured. This is the reason for the term “remote field eddy currents” (as opposed to the near or direct field currents from waves propagating down the bore of the pipe).

This is exactly what is needed. Any pipeline flaws such as metal loss from corrosion or other causes that affect the propagation of these RFECs back into the pipe alter the detected signal so that the flaws may be detected and measured by the sensing coils.

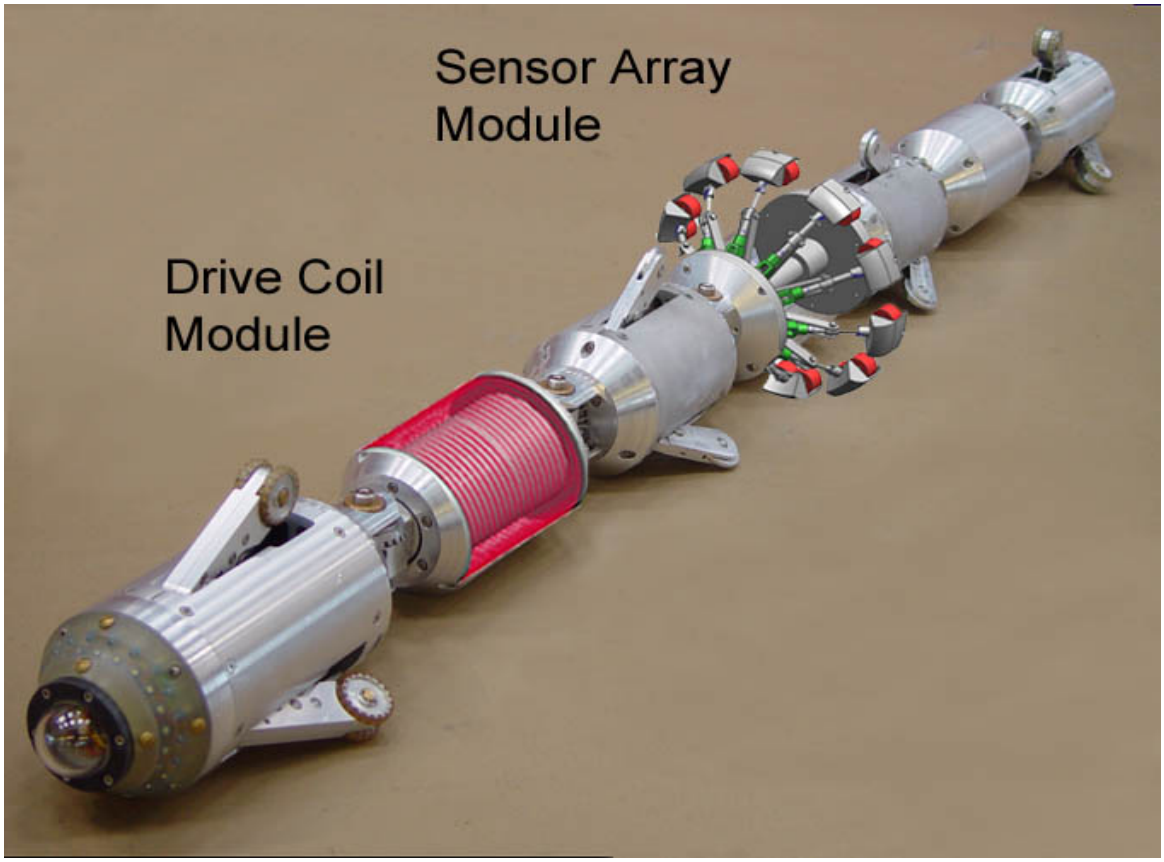

Figure 2: A drawing simulating the RFEC technology integrated to the Explorer I robot.

The RFEC frequencies need to be low since higher frequencies will not penetrate ferromagnetic conductors such as pipeline steel. Methods to increase penetration by lowering the magnetic permeability by magnetizing the pipe may not work well for unpiggable pipelines for the some of the same reasons that MFL inspection will not work well. The one disadvantage of the technique will therefore be slow inspection speeds. Other than that, the RFEC technique is the ideal in-line inspection technology for inspecting “unpiggable” pipelines. The transmitter and sensors can be designed to fit through anything that robots or any design of pig driving cups can pass through. Figure 2 shows a conceptual design for the proposed inspection device using Explorer II to propel the tool through a distribution main. The transmission coil can be much smaller than the pipeline diameter and mounted on a short module. Power and electronic modules, including possibly a recharging module, can be mounted ahead and between the

transmitter and the sensors with additional modules, if needed, following behind these. Modules at each end of the RFEC in-line inspection tool can move the tool in either direction.

NON EXPERIMENTAL

GTI completed the Research Management Plan. The plan detailed the work to be performed as outlined in the Statement of Objectives and included the project schedule and staffing. The work will consist of three phases, Design, Construction, and Integration and Demonstration. GTI completed the Technology Assessment Report that described both the status of the RFEC technology and where it fit within available technologies for enhancing pipeline reliability. The feasibility of inspecting transmission pipelines using the RFEC technique was proven in a previous DOE project (DE-FC26-02NT41647). The technique can use small components making it ideal for its primary purpose of inspecting unpiggable pipe. The current project will demonstrate that capability in an operating pipeline or distribution main.

We have completed all Task 3.0 deliverables, which include anticipated constraints, protocols, and requirements. Based on the group sensor/platform definition activities in Task 3.0, we drafted initial requirements for the sensor module thereby completing the deliverables for Task 4.0. Tasks 6.0 and 7.0 deal with advanced sensor module design. Task 6.0 was the Mid-Phase Design Review. For this task, we presented preliminary designs for the sensor module. We provided a detailed review of system specifications and of key parameters for successful integration. We presented three sensor module designs at the review meeting. These designs were developed at GTI through brainstorming and 3D modeling activities. The mid-phase design review was originally scheduled midway through Phase I but was pushed back because the overall program schedule fell behind. Consequently, the Final Design Review, Task 7.0, has not taken place at this time. GTI is prepared to participate in the Final Design Review. We have made our final choice for the sensor module design and are currently in the process of packaging the module. This includes specifying gearing, determining and maximizing the amount of space available for electronics, and strengthening the modules, etc. Another design improvement we are working on is providing compliance to the arms for passing through areas of ovality and being able to handle moments of robot sag. Along with mechanical design, Task 7.0 also requires a review of system specifications and key parameters. We have developed electronic schematics and specifications for our modules. We also developed a set of Sensor Module Commands in UML (Unified Modeling Language) to facilitate exchanging information and commands over the Explorer II CANbus.

EXPERIMENTAL

Figure 3: RFEC laboratory setup.

Figure 3 shows the laboratory setup for performing RFEC research tasks. We machined defects sets into two 10' sections of 6" diameter pipe. One pipe is seamless, the other is seam welded. The seamless pipe is set up with a Kepco BOP, bipolar operational power supply, on the right, which drives the exciter coil and a PerkinElmer lock-in amplifier, on the left, which filters and amplifies the signal received by the sensing coil.

Originally, we started with an exciter coil made of 1000 turns of #29 copper wire wound 2" wide on a 1 ½" diameter spool. Electromagnetic waves for the remote field were generated by driving the coil at 8.6 V rms and 0.2 A rms by the BOP. The sensing coil was made of 20,000 turns of #46 copper wire wound on a 3/8" wide, ¾" diameter bobbin. The output of the sensing coil is filtered and amplified by the lock-in amplifier. The lock-in amplifier rejects all frequencies except that of its internal oscillator. The internal oscillator of the lock-in amplifier provides the signal that is amplified by the BOP to drive the exciter coil.

Figure 4: RFEC testing on 12” pipe samples.

Early in the project, we performed RFEC testing on 12” seamless and seam-welded pipes. Figure 4 shows the pipes and equipment tent. This testing was initially started in preparation for the DOE-NETL technology demonstration held at Battelle Laboratories in Ohio. The RFEC vehicle is shown in Figure 5.

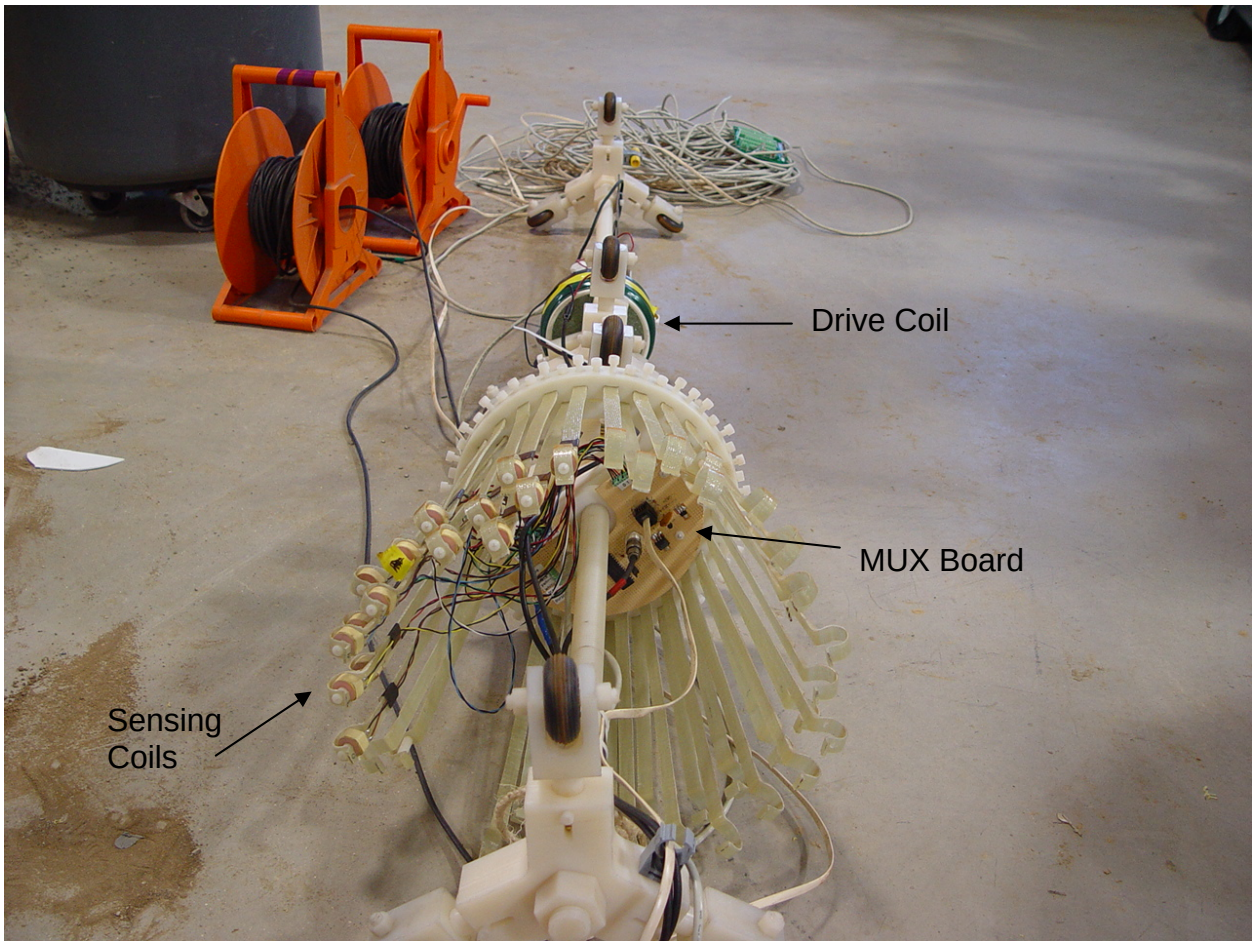

Figure 5: Testing vehicle for RFEC inspection of 12” pipes.

ELECTRONICS and DATA ACQUISITION IMPROVEMENTS

The vehicle features a 16-channel multiplexing board, MUX to be able to acquire data from 16 sensing coils. We also built a 16 channel MUX for use on the 6” pipes in the laboratory. In order to collect data for 16 sensor coils, we updated our LabVIEW data acquisition program to step through and record data from all 16 channels. In addition to sensor data, the addition of odometry to the vehicle required the LabVIEW program to also record position data from the odometer at acquisition locations.

Using the MUX board and LabVIEW significantly improved collection speeds. Manually, it would take close to two hours to inspect a single defect. Using the new system, all 13 defects along a 10’ section of pipe can be inspected in an hour and a half without a researcher present. Further improvements in inspection speeds were seen when GTI purchased a Ferroscope and

software from Russell Technologies, Inc. This is a much more sophisticated system as Russell has years of experience using the RFEC technique to inspect boiler tubes. The collection speeds on this setup are about 3 minutes for a 10’ length of pipe.

LAB APPARATUS

We’ve also made improvements in the 6” vehicle. The original vehicle had one coil mounted on an arm. To be able to mount multiple coils, we drilled equally spaced holes into a 6” disc and mounted three sets of 5 coils each at 120° locations. This new vehicle allowed us to scan all the defect sets at the same time using the BOP and lock-in setup. We also installed a motor-encoder mechanism to automate the data collection. In addition, a self-righting mechanism was put in place to prevent major rotations of the vehicle. This eliminates the need to “uncurl” the data during analysis.

GEOMETRIC & SYSTEM STUDIES

We have studied drive and sensor coils separation distance as a function of frequency. We obtained understandable results up to the 1-2 kHz range in frequency. We also studied defect detection at a set frequency as a function of sensor orientation to pipe axis. The results of these studies are discussed in the results section of this report. We also studied multiple exciter coils in both the 12” and 6” pipes. These studies have enabled us to reduce power consumption, which is important for use on the Explorer II robot which has limited power.

RESULTS AND DISCUSSION

WORK PERFORMED ON 12” PIPE

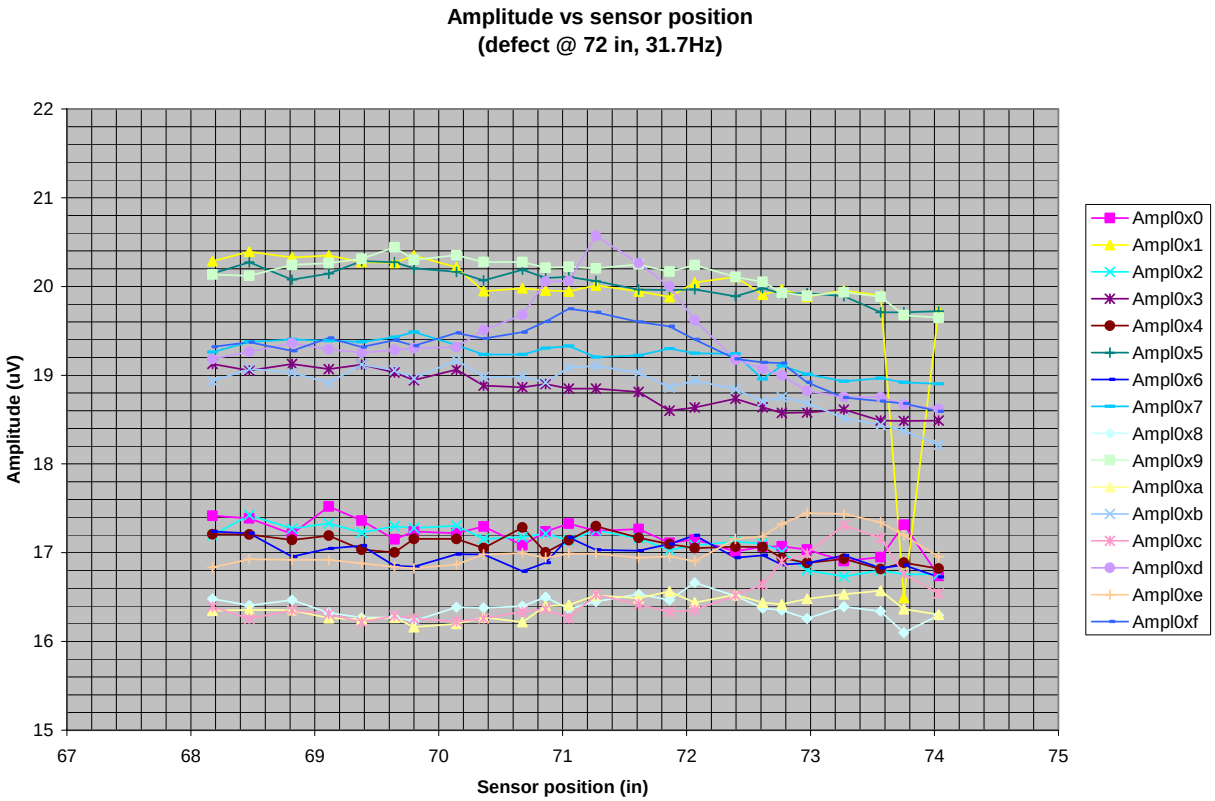

Figure 6: Amplitudes vs. Sensor Position Inside 12” Pipe

The graph in Figure 6 shows the amplitudes of the signals seen in all 16 channels while scanning a 6” section of the 12” test pipe. The 80% WT defect is nominally at 72” from the end of the pipe. The sensors labeled *Ampl0xd, Ampl0xf, Ampl0xc,* and *Ampl0xe* all indicate an increase in amplitude near the defect location. The horizontal axis indicates the position of sensors *Ampl0xd* and *Ampl0xf* along the pipe. *Ampl0xd* and *Ampl0xf* do not indicate exactly 72” because of systematic and correctable imprecision in their position. This is not due inherently to the technique but rather to position calibration constants. Due to mechanical constraints, the sensors *Ampl0xc,* and *Ampl0xe* are about 2” farther into the pipe[1], which is why they indicate a defect location about 2” farther than the other two sensors. The fact that multiple sensors

1 This 2” separation between adjacent sensors is visible in Figure 5.

indicate the defect allows for locating it circumferentially as well as axially.

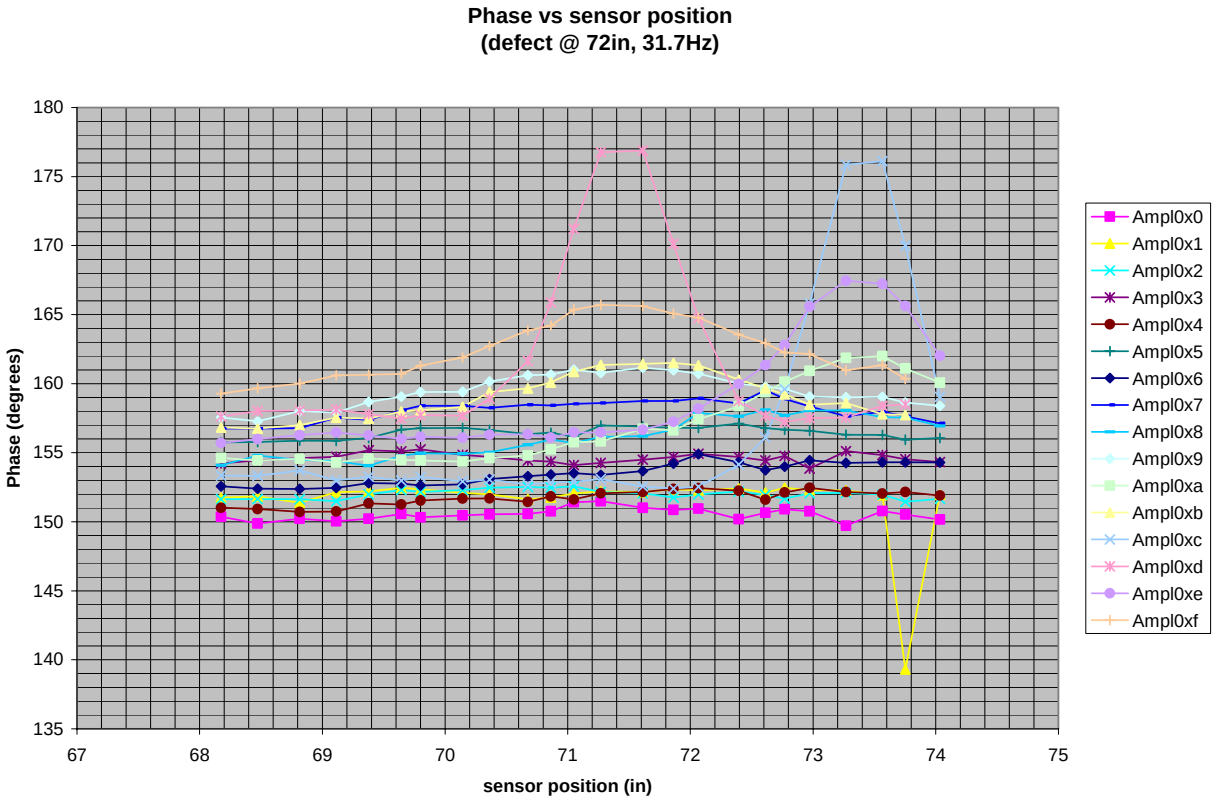

Figure 7: Phases vs. Sensor Position Inside Pipe

Figure 7 shows the phases of the signals seen in all 16 channels while scanning a 6" section of the 12" test pipe. The 80% WT defect is nominally at 72" from the end of the pipe. The sensors labeled *Ampl0xb, Ampl0xd, Ampl0xf,* and *Ampl0xa, Ampl0xc, Ampl0xe* all show an increase in phase near the point of the defect. The horizontal axis indicates the position of sensors *Ampl0xb, Ampl0xd, Ampl0xf*. The defect signals on channels *Ampl0xb, Ampl0xd, Ampl0xf* do not occur exactly at 72" because of systematic and correctable imprecision in their position. This is not due inherently to the technique but rather to position calibration constants. Due to mechanical constraints, the sensors *Ampl0xa, Ampl0xc, Ampl0xe* are about 2" farther into the pipe, which is why they indicate a defect location about 2" farther than the other two sensors. The fact that multiple sensors indicate the defect allows for locating it circumferentially as well as axially.

The graphs in Figures 6 and 7 are simple excel plots. One advance made in this segment

of the project was the purchase of Adept Pro software from Russell Technologies. Figure 9 shows a screenshot of Adept Pro.

The Adept Pro display shows a strip chart of the phase angle on the left (ignore the analysis functions on the far left), followed by a C-Scan of the phase. Although the C-Scan provides a good overview of the defects, often as in this case, the strip chart is better for seeing the smaller defects. The magnitude information is displayed to the right of the phase information. The top right hand panel shows the Voltage Plane. The black spiral is the attenuation spiral: as the wall thickness increases, the remote filed eddy current signal strength decreases while the phase also decreases, resulting in a spiral in a polar plot. The blue curve on the plot is the signal from the defect at the marker that runs across the strip charts and C-scans. The two red lines on either side of the marker mark the range of data analyzed. The angle between the blue line and the spiral determines the defect depth, while the distance to the intercept with the attenuation spiral indicates the circumferential extent of the defect.

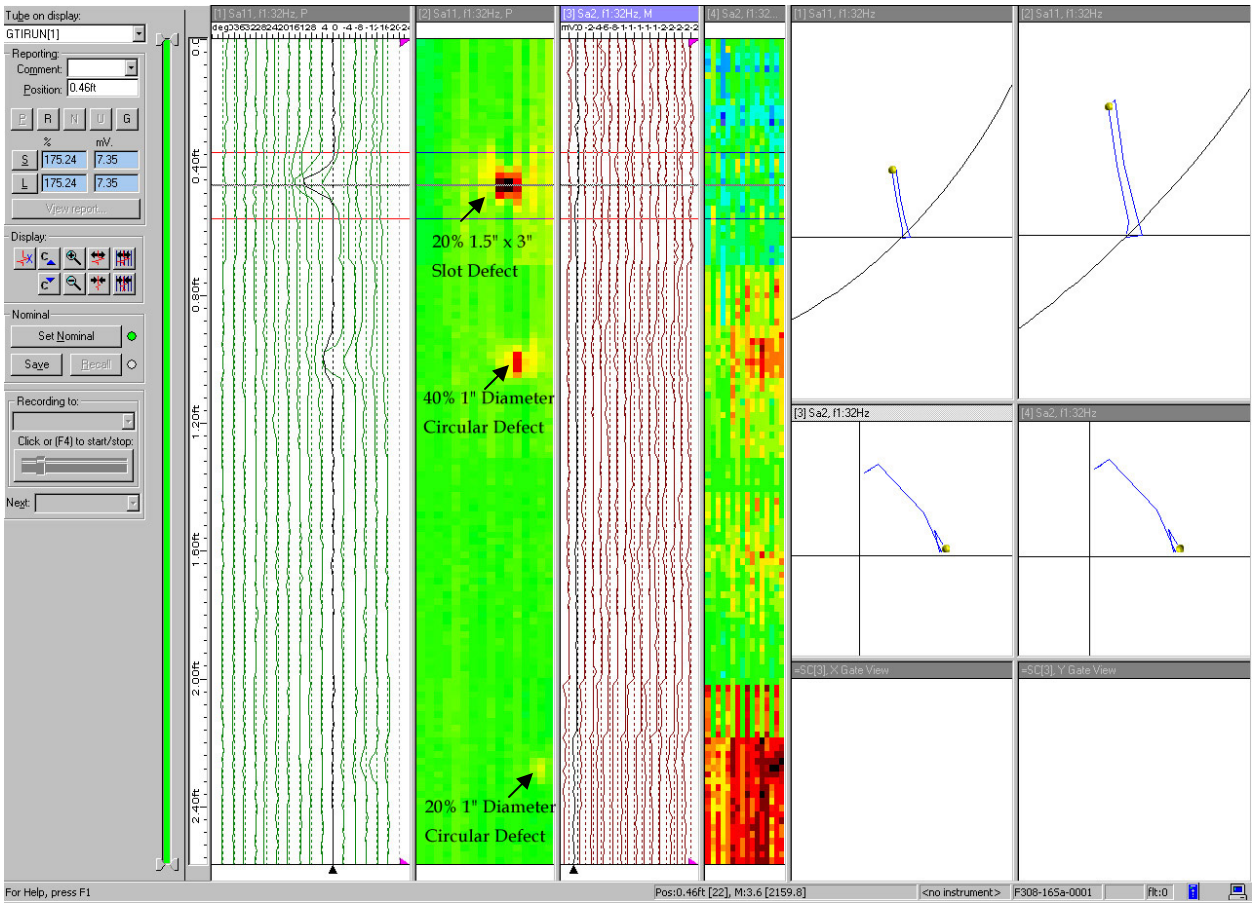

Figure 8: Screenshot of Adept Pro software showing defect locations in pipe.

Figure 8 is data analysis done on one defect line of a 12” seam welded pipe. Three of four defects were identified. The defect that was not detected was a 1” diameter circular defect of only 10% of the wall thickness.

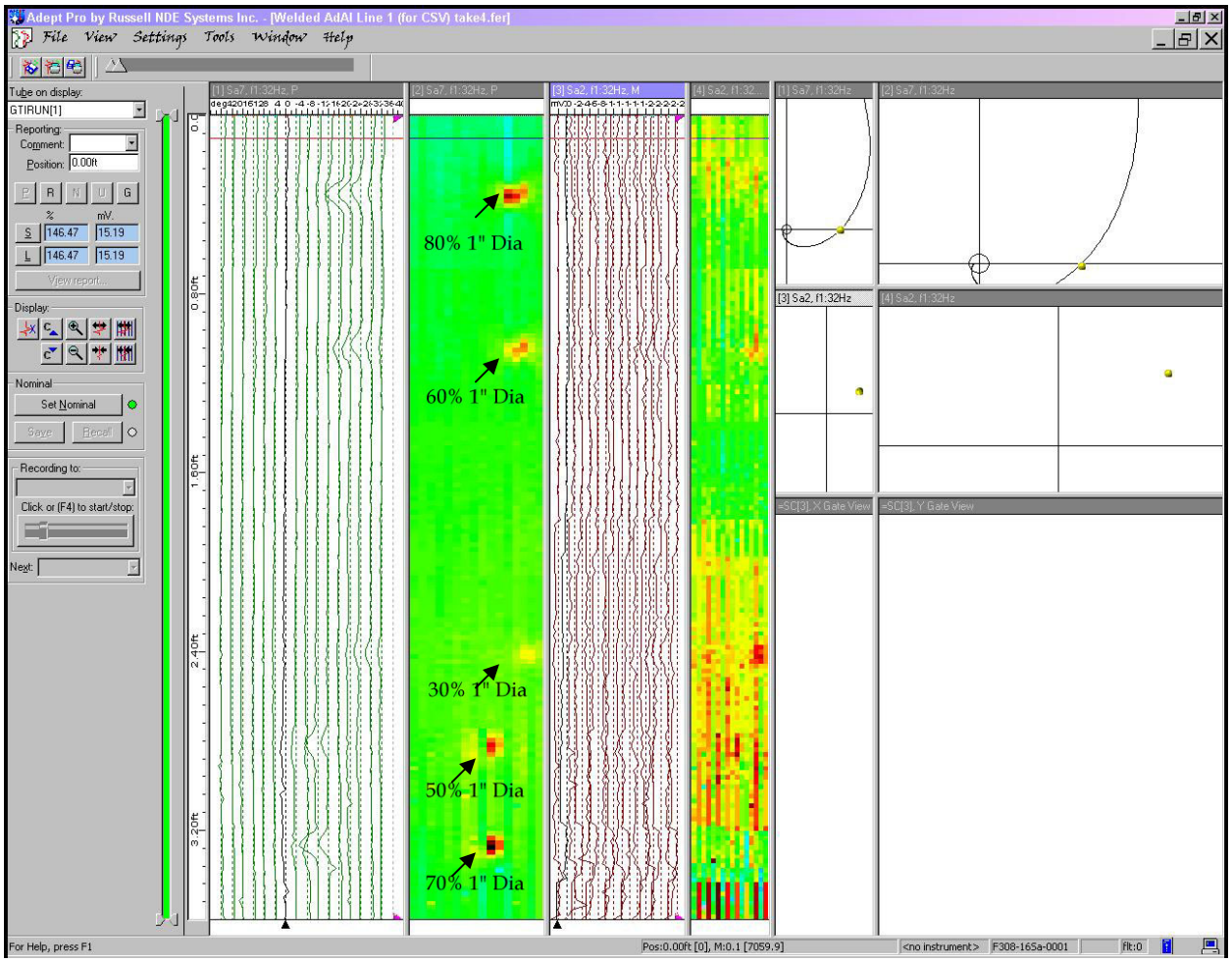

Figure 9: Adept Pro software showing defect locations in pipe along defect line 1.

Figure 9 is data analysis done on the first defect line of a 12” seam welded pipe with the second drive coil. Five of six defects were identified. The defect that was not detected was a 1” diameter circular defect of only 5% of the wall thickness.

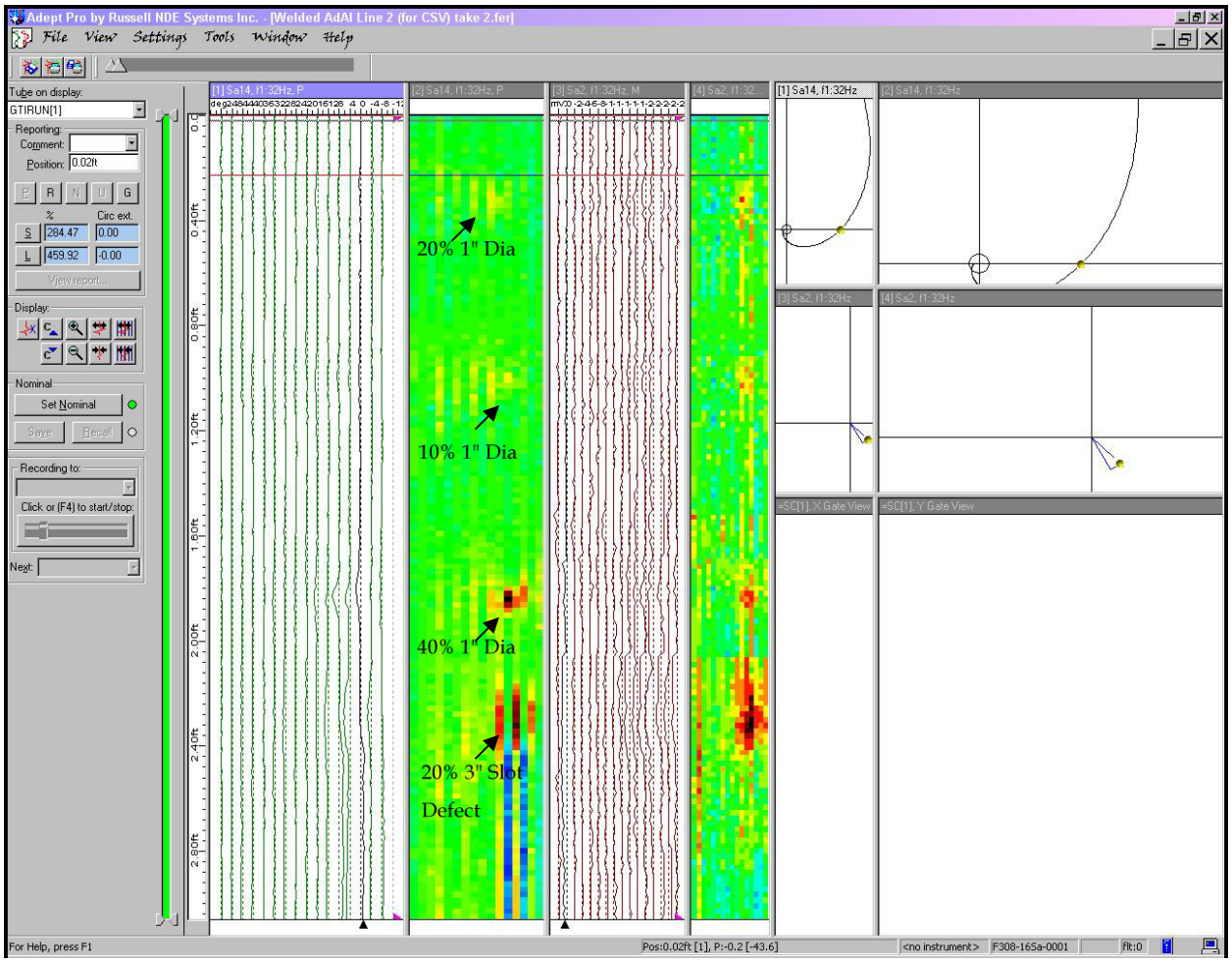

Figure 10: Adept Pro software showing defect locations in pipe along defect line 2.

Figure 10 is data analysis done on the second defect line of a 12” seam welded pipe with the second drive coil. Four of four defects were identified. The smallest defect that was detected was a 1” diameter circular defect of only 10% of the wall thickness.

WORK PERFORMED ON 6” PIPE

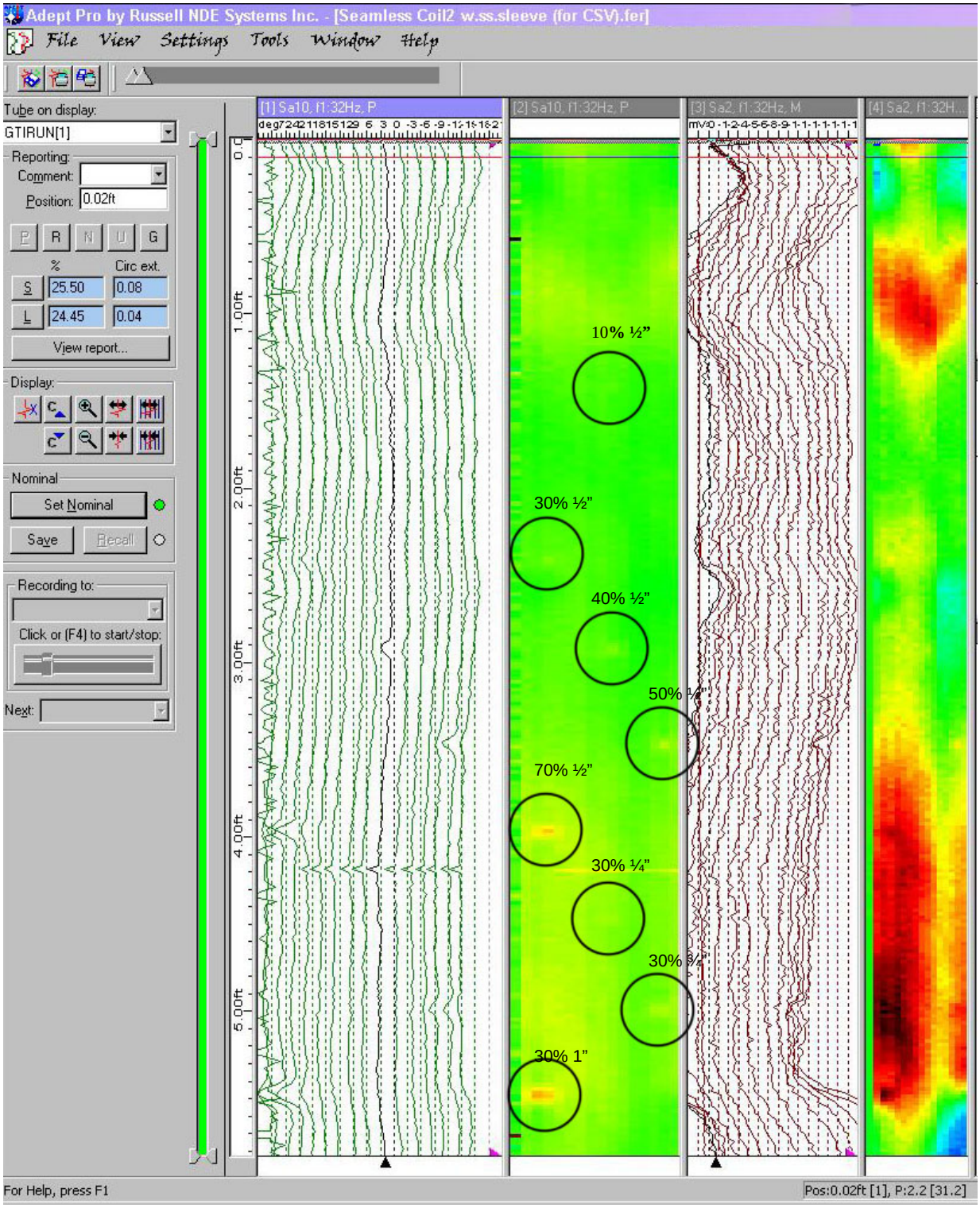

Figure 11: Screen shot of 6” seamless pipe scan from Adept Pro Software.

Figure 11 is a scan of the entire 6” seamless pipe. During this test, a stainless steel sleeve, was placed between the exciter and sensor coils. We were testing the effect of metal components on detection results since the Explorer II robot is metallic. Our concern is that the metal could disrupt the electromagnetic fields and produce poor results. In actuality, we obtained better results with the sleeve inserted. This scan covered 10 defects. Eight of them are identifiable in the strip chart to the left of the screenshot. The two defects that did not show in the data were a 5% ½” and a 30% ¼” defect. We suspect the 30% defect was not detected because we scan in ¼” steps. It is likely that we stepped right over that defect. The results seem to be very promising as the 10% ½” defect was found. We repeated this test with a chunk of aluminum of 3” diameter and 3” in length. The results were slightly noisier but there was no apparent drop in the amplitude of the signal. The smallest defect detected in this run was a 30% ½” round.

After completing the above testing with metal components, we performed a study of differential coils. Our differential coils consisted of two identical coils mounted close to each other on the same axis and were operated with each coil 180° out of phase with the other’s current. Data analysis included taking the absolute measurement of each coil then subtracting them to get the differential. Results of scanning the pipe along all three defect lines of the 6” seamless pipe are shown in Figure 12. The absolute measurements are plotted in red and orange and the differential measurement is plotted in yellow. The bright red vertical lines represent defect locations along the length of the pipe. The defects measured absolutely are indicated by significant increases in amplitude. A sharp drop followed by a sharp increase in amplitude indicates differential defects. These can be seen in Figure 12. The most obvious is the 80% deep defect located around 78” on Line 1. Because of the length of the RFEC vehicle, we were unable to scan the entire pipe in one pass. For each coil tested, we turned the vehicle around and ran it through from the other end of the pipe. These results are not represented in this report. The differential coils do not appear to have any significant advantage over our standard sensor coils.

DIFFERENTIAL COIL TESTING

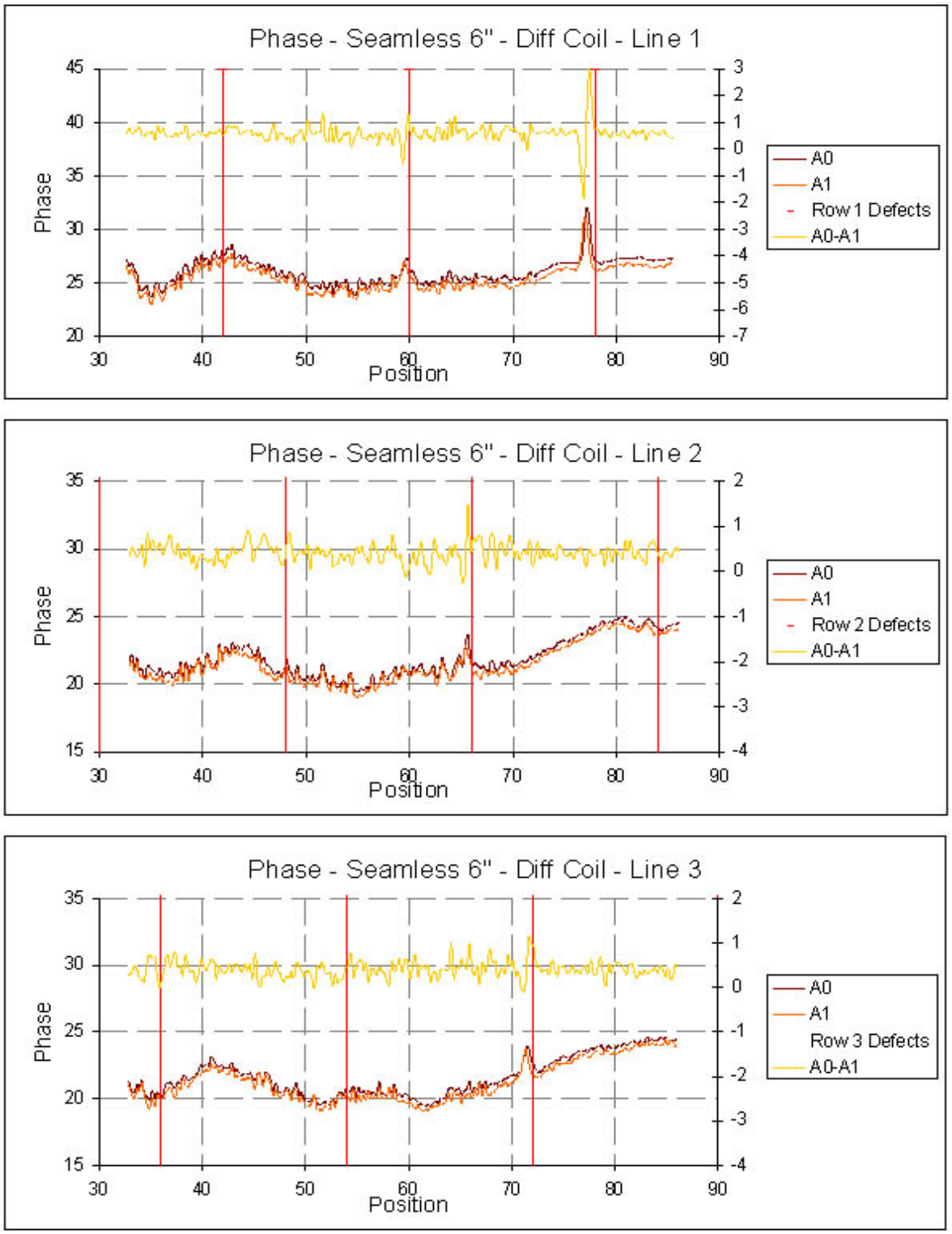

Figure 12: Results of scanning the 6” seamless pipe with differential coils.

Before beginning testing with Coil 5, we made an improvement in the laboratory setup. We attached a 4’ section of 6” PVC pipe to the starting end of the seamless pipe. The PVC pipe has large windows cut out of it to facilitate changing components on the vehicle. It also allows us to start taking measurements from the zero mark rather than starting at 33". This lets us inspect the defects located at 24” and 30” without pulling the RFEC vehicle through from the other end.

In addition to coil testing, we standardized our exciter coil - sensor coil center-to-center distance to 15” based on the dimensions of the Explorer II. Prior to this standardization, the center-to-center distance for each test was based on pullout results of the individual exciter coils.

EXCITER COIL 5 TESTING

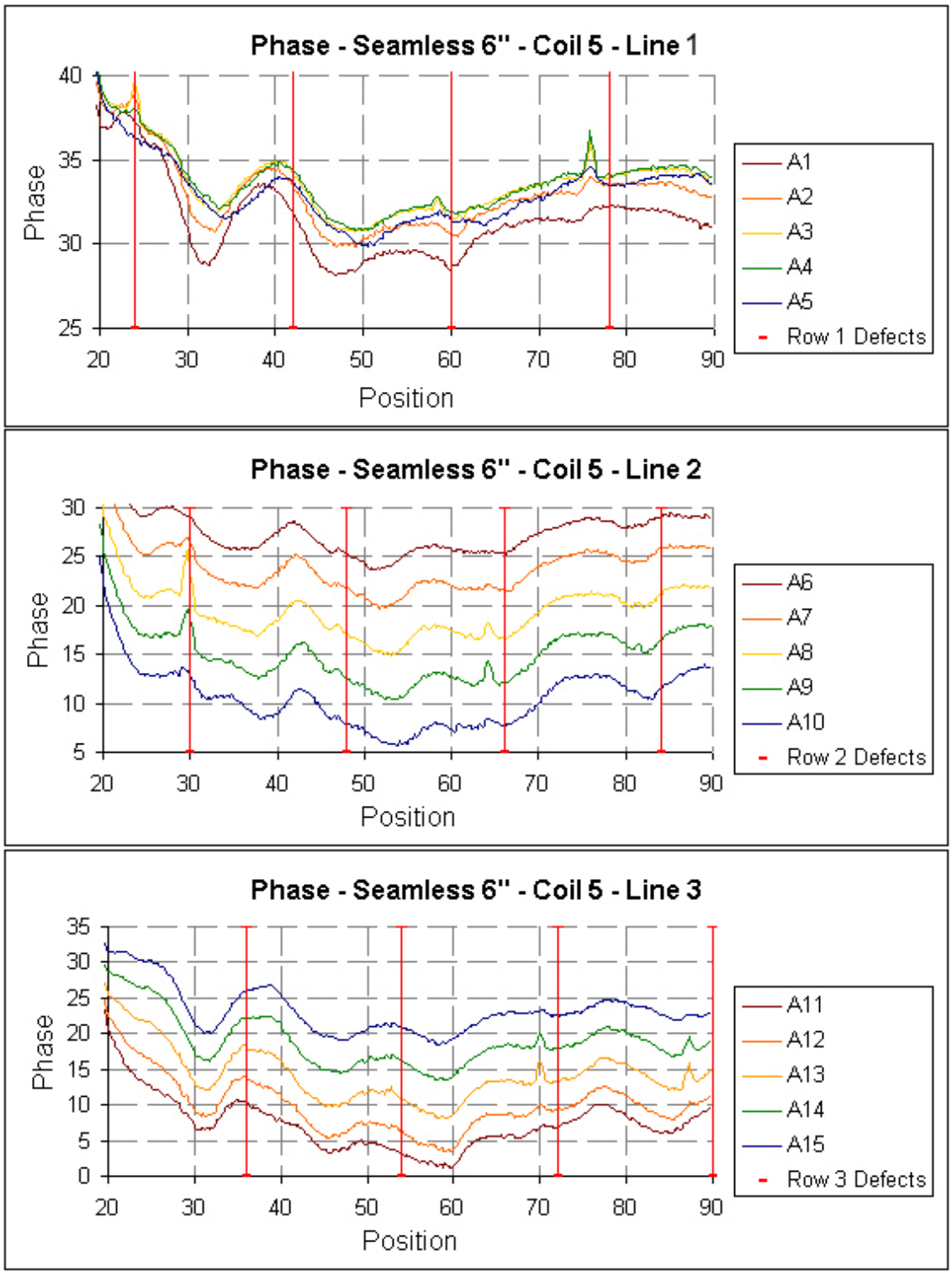

Figure 13: Results of 6” seamless pipe scan using Coil 5 with a mock module.

Figure 13 shows the results of scanning the 6” pipe with Coil 5 as the exciter coil. This test was performed with an imitation aluminum Explorer module between the exciter coil and pick-up coils. This test was conducted to ensure that the metal module would not cause an intolerable disruption of the RFEC signals. We were pleased with the results in Figure 13. The defect locations are marked with red vertical lines. An increase in the phase can be seen in at least one coil at most defect locations. The defects that were not detected are the 5%, ½” at 42” in line 1, the 30%, ¼” at 36” in line 3, and the 20%, ½” at 54” in line 3. None of these defects would be repaired in the field.

EXCITER COIL 6 TESTING

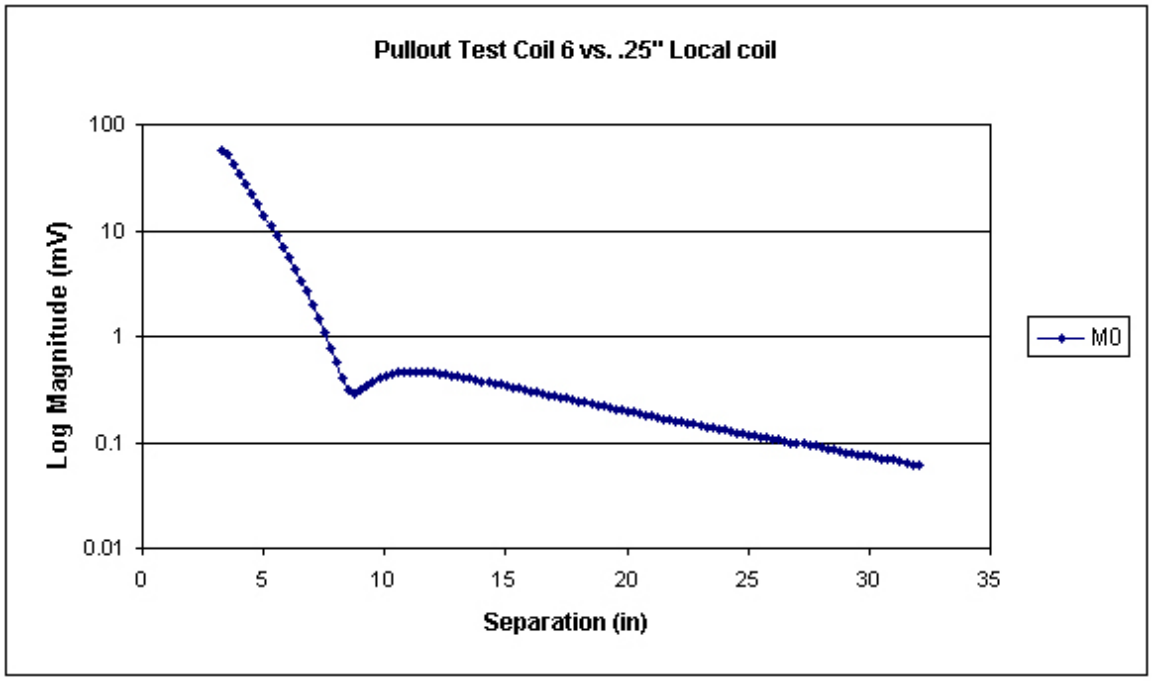

Figure 14: Results of a pullout test using Coil 6.

Upon completion of winding Coil 6, we performed a pullout test. The pullout test consists of starting the exciter coil and sensor coils close together and taking readings as they are pulled away from each other. The test shows where the direct field attenuates and the remote field signals will be the only detected signals. The log plot of the magnitude in Figure 14 shows the pick-up coils should be positioned at least 11” away from exciter coil 6. The strength of the signal remains strong through about 20”. Following the pullout test, we scanned the 6” seamless pipe using Coil 6. The results are shown in Figure 15.

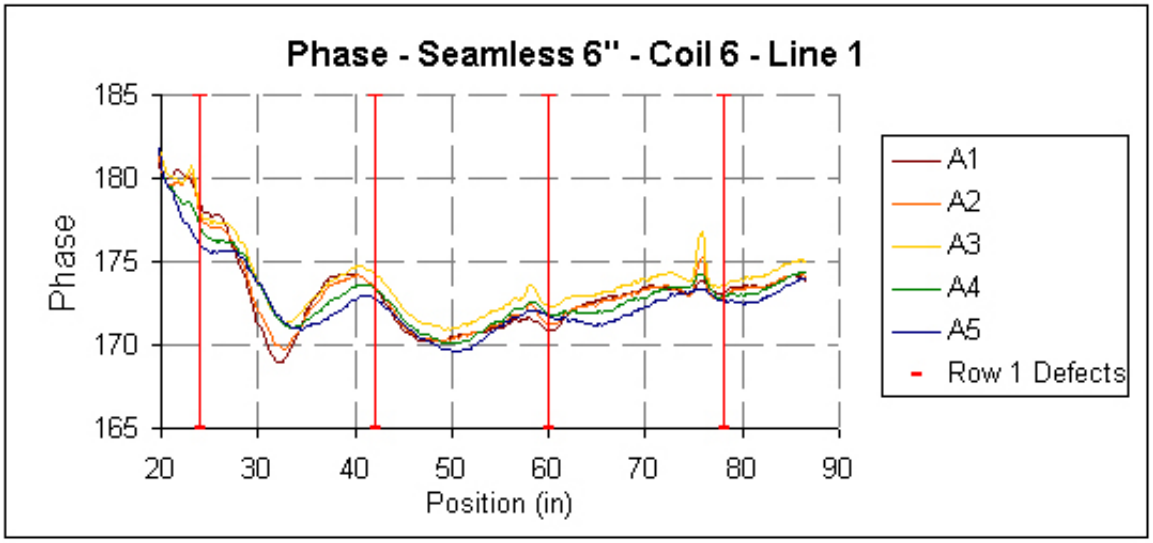

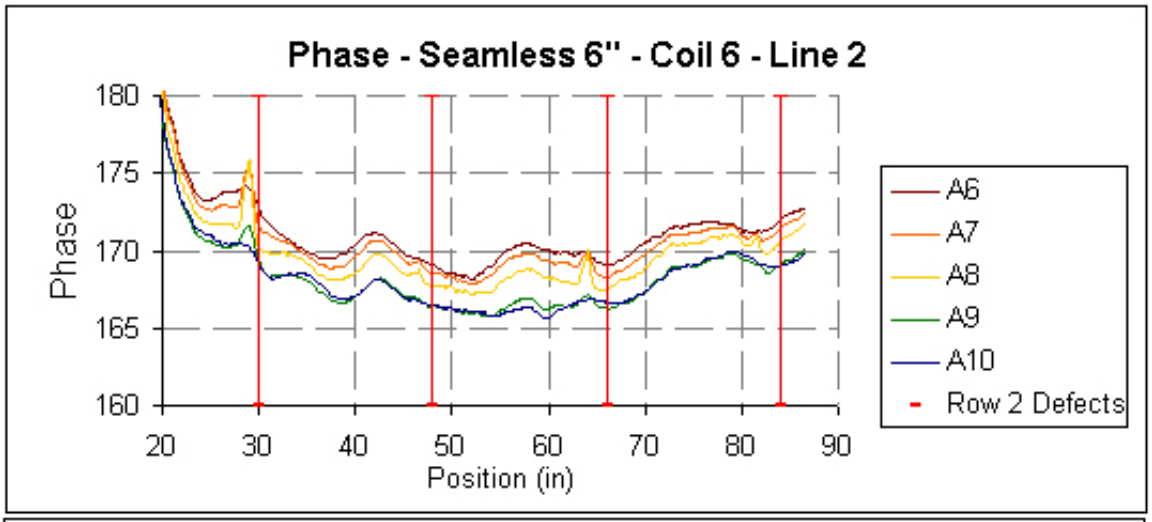

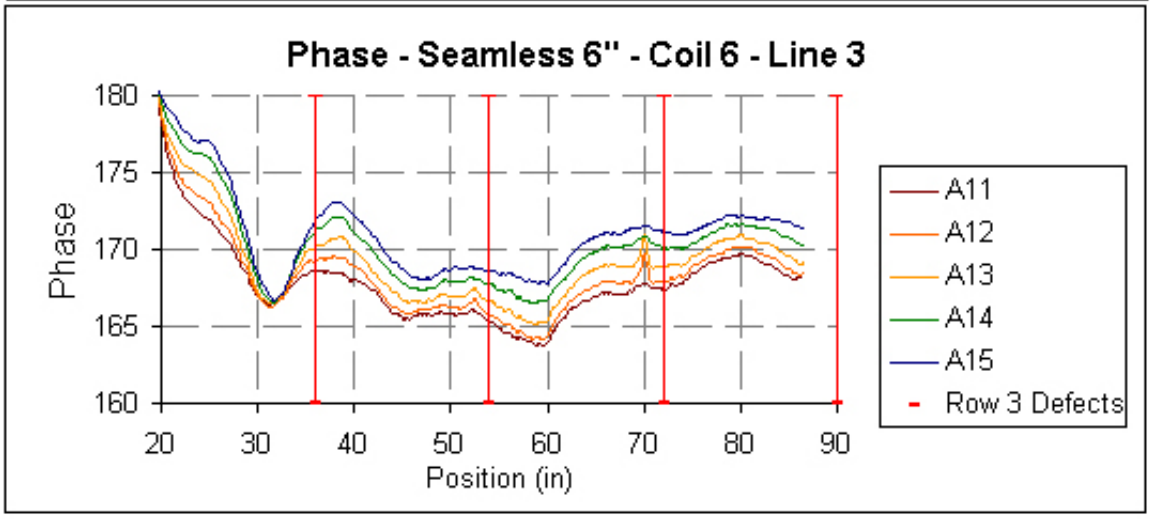

Figure 15: Results of scanning the 6” seamless pipe with Coil 6.

The figure above shows scanning results of exciter coil 6 in the 6” seamless pipe. The results are similar to Coil 5 results shown in Figure 13. Coil 6 detected all the defects Coil 5 and in addition, detected the 20%, ½” defect at 54” in line 3. In other scans with Coil 6, we have seen detection of all defects with the exception of the 5%, ½” defect.

EXCITER COIL 7 TESTING

Coil 6 is made from 900 turns of wire across 4” of a 3.5” diameter roll. We modified the geometry by winding the same number of turns across 2.5” of a 3.5” diameter roll. This is Coil 7. Theoretically, the shorter exciter coil, 7, should have a quicker attenuation of the direct field because the propagating fields are less spread out across the length of the coil. We performed a pullout test on Coil 7 as we did with Coil 6.

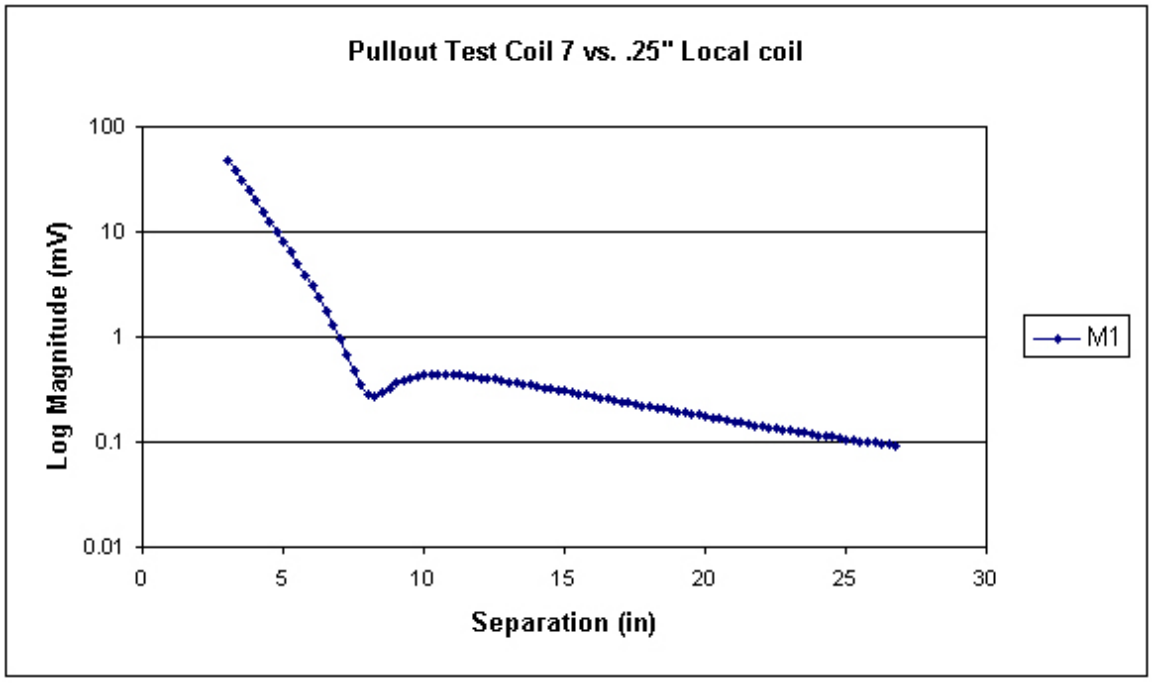

Figure 16: Results of a pullout test using Coil 7.

As we expected, the sensor coils can be positioned closer to the exciter Coil 7 than Coil 6. The sensor coils should be placed at least 10” from Coil 7 for inspection. This is 1” closer than Coil 6 placement relative to the sensor coils. Results of the pullout test for Coil 7 are shown in Figure 16.

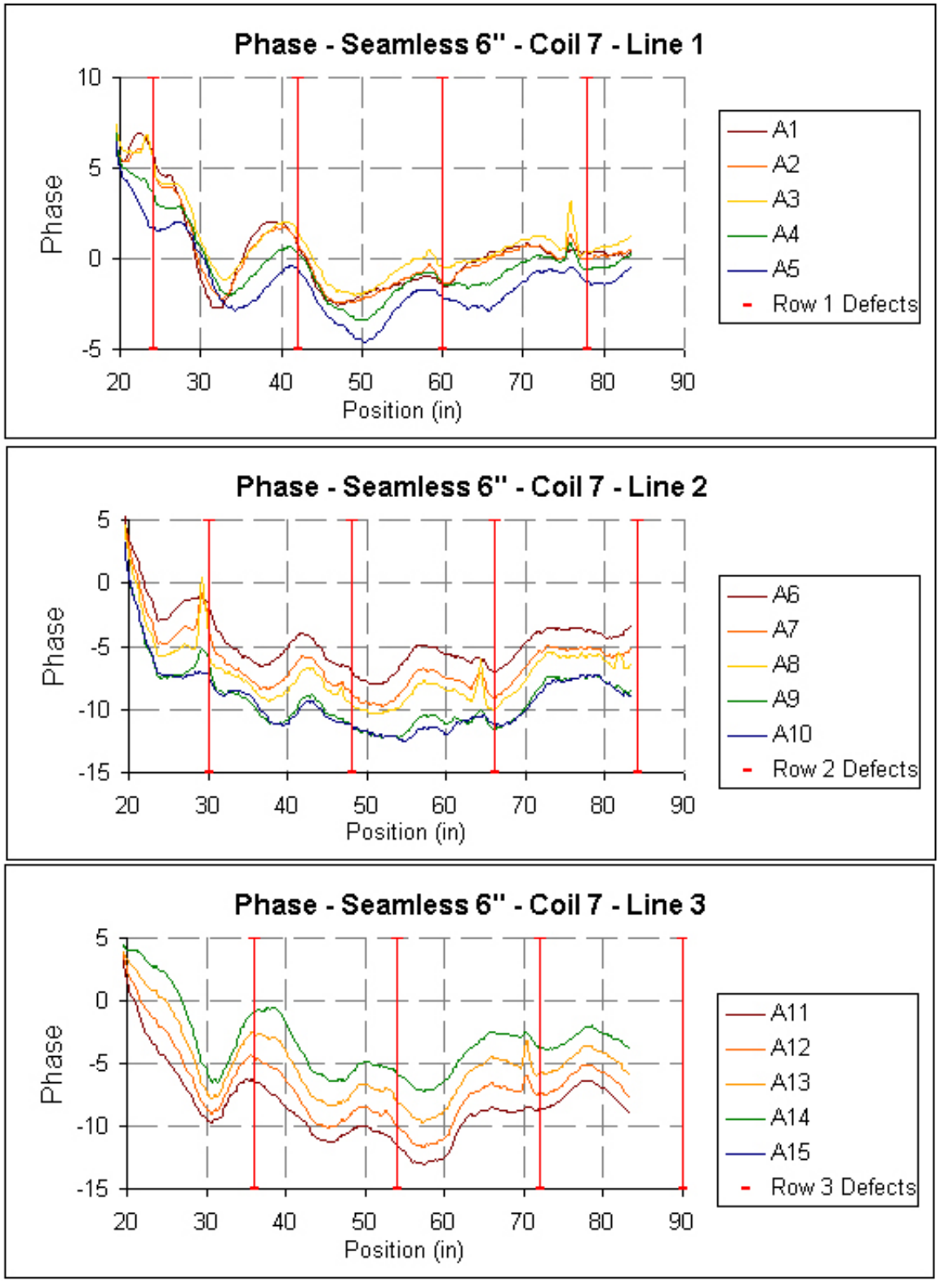

Figure 17:Results of scanning the 6” seamless pipe with Coil 7.

Figure 17 shows results obtained from scanning the 6” seamless pipe with Coil 7 as the exciter coil. To date, Coil 7 has been the only exciter coil to detect all 13 defects, including the 5% wt. Throughout the testing process, the data obtained from scanning the seamless pipe tends to follow the same trends. At the same time, there are also trends in the magnitude and phase data from the welded pipe scans. The patterns in the welded pipe differ from the patterns seen in the seamless pipe. We suspect the gradual rising and falling of the data is attributed to residual magnetic fields in each of the pipes. In order to better understand the data and to have a set of data to use as the base, we set up a baseline test. We laid both pipes parallel to each other and ran subsequent tests using the same vehicle and lab equipment. The first baseline test results are displayed in Figure 17. We performed the first scan on the seamless pipe. Upon completion of that scan, we transferred the RFEC vehicle to the welded pipe and performed a new scan on the welded pipe. These results are shown in Figure 18 below.

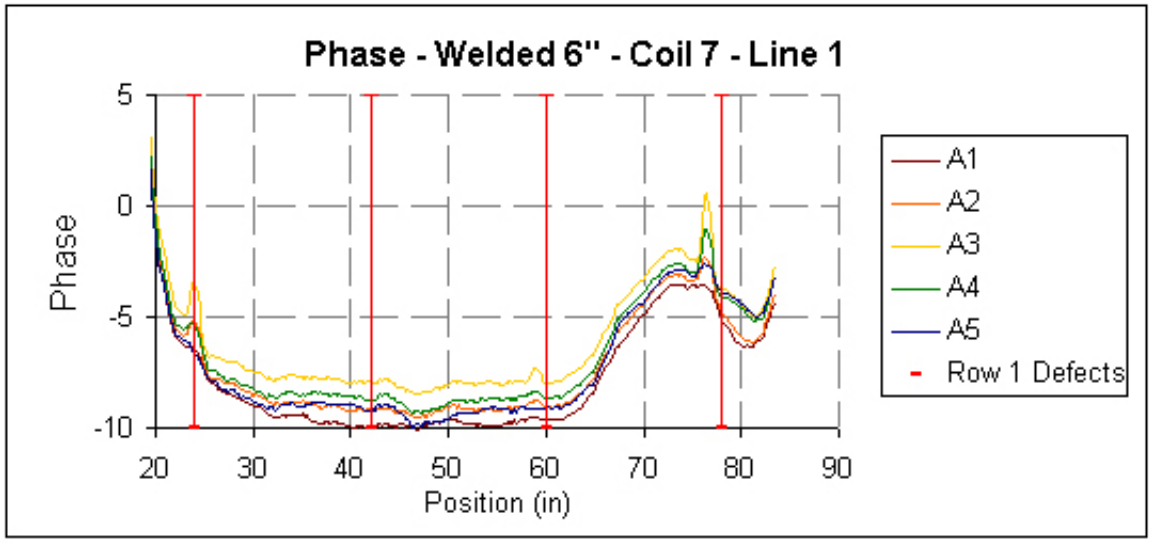

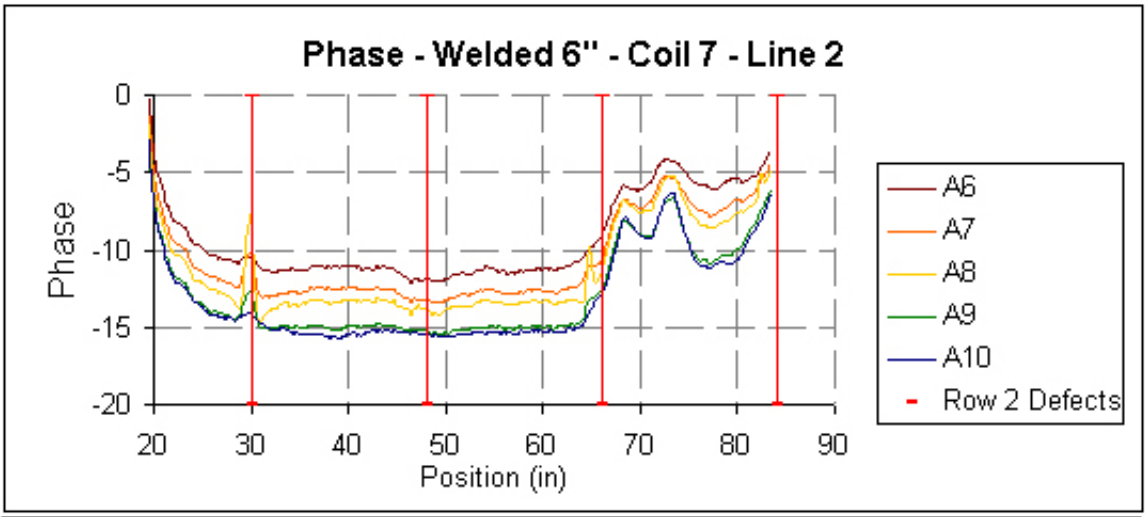

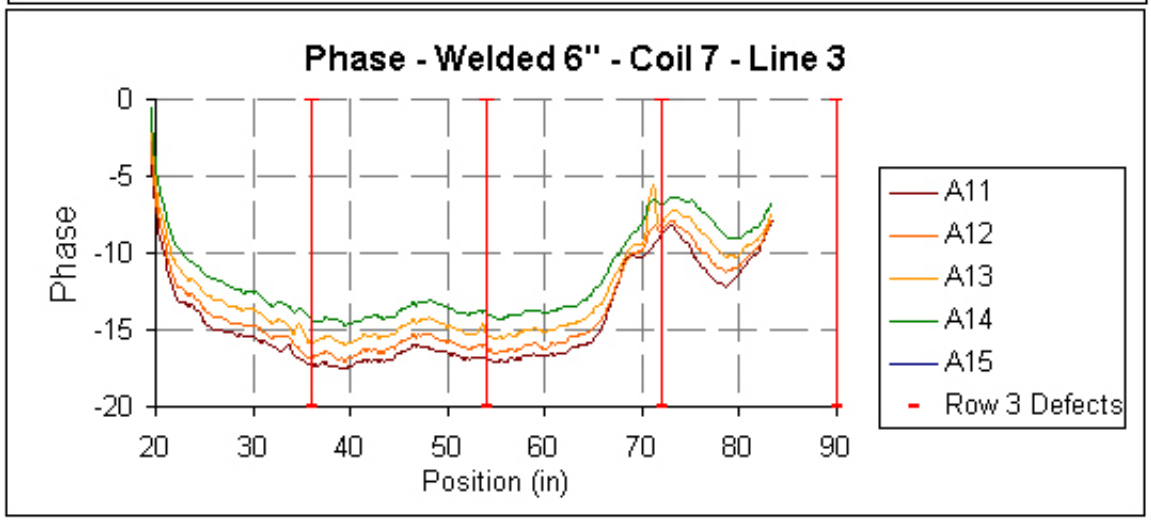

Figure 18:Results of scanning the 6” welded pipe with Coil 7.

ASSESSMENT OF EXCITER COILS

Table 1 below is a listing of all the defects, their location, depth, diameter, and shape as well as the detection ability of each of the coils. Check marks represent if the defect was detected. The X's represent the defect as not being detected by that particular coil. Coil 7 was the only exciter coil to detect all the defects. Coil 6 was able to detect all but the 5%, ½" defect. Coils 2, 4, and 5 were able to detect the 20%, ½" defect but did not detect the 30%, ¼" defect. The reason the 30% was not detected is that the diameter is only ¼" and we scan the pipe in ¼" steps. Most likely, the defect would be detected scanning in 1/8" steps. All in all, any of these exciter coils are sensitive enough for accurate detection of defects in an operating pipeline that would require repair.

Row	Location	Depth	Diam.	Shape	Coil 2	Coil 4	Coil 5	Coil 6	Coil 7
Row 1	24"	30%	1"	Round	✔	✔	✔	✔	✔
	42"	5%	½"	Round	✘	✘	✘	✘	✔
	60"	30%	½"	Round	✔	✔	✔	✔	✔
	78"	70%	½"	Round	✔	✔	✔	✔	✔
	96"	30%	1"	Square	✔	✔	✔	✔	✔
Row 2	30"	30%	¾"	Square	✔	✔	✔	✔	✔
	48"	10%	½"	Round	✔	✔	✔	✔	✔
	66"	40%	½"	Round	✔	✔	✔	✔	✔
	84"	30%	¼"	Square	✔	✔	✔	✔	✔
Row 3	36"	30%	¼"	Round	✘	✘	✘	✔	✔
	54"	20%	½"	Round	✔	✔	✔	✔	✔
	72"	50%	½"	Round	✔	✔	✔	✔	✔
	90"	30%	¾"	Round	✔	✔	✔	✔	✔

Table 1: Ability of drive coils to detect various sized defects

Choosing the proper exciter coil for use on the Explorer II will be more involved than just selecting the coil with the best detection ability. It is important for the coil to make good use of available module space. Additionally, limiting weight and power consumption will be critical.

To date, we have tested a total of five exciter coils, 2, 4, 5, 6, and 7.The specs for these coils are listed in Table 2 below. Of the five, Coil 4 was the most undesirable because of its power consumption and size. Coil 2 is also undesirable based on size relative to the size of the

robot module. We wound coils 5-7 around a 3.5” spool to make better use of the module space. The inner diameter is large enough to fit electronic components inside of it yet small enough to wrap it with a protective shield for use in the pipeline. Coils 6 and 7 are rather heavy but were able to detect more defects than the other exciter coils. Coil 5 is a likely candidate because it strikes a good balance between the trade off of weight and power consumption.

Coil Name	Inner Diameter (“)	Length (“)	# of Turns	Wire Gauge	Weight (lb)	Power Consumption (W)
Coil 2	2.375	3.25	2000	29	1.03	1.06
Coil 4	2.375	1	750	29	.35	6.62
Coil 5	3.5	4.25	1355	26	1.85	1.85
Coil 6	3.5	4	900	28	3.76	2.35
Coil 7	3.5	2.5	900	28	3.09	4.11

Table 2: Specifications of exciter coils tested.

RUSSELL FERROSCOPE

Preliminary tests were conducted with the Russell detector boards in the welded 6 inch pipe. The Russell boards output information in in-phase and quadrate components. A computer program was written to convert the data into amplitude and phase format for analysis. The program also allows the option to scale the data (necessary for use in the Russell data analysis program) and to average data over a fixed time length (useful for reducing noise levels and comparing data with the original lock-in amplifier).

The results of the first test shown in Figure 19 below are for two coils pulled at a rate of about 1.5 inches/second. The complete defect line was scanned in 100 seconds compared to the lock-in amplifier which took about 90 minutes. The length of the lock-in scan is due mostly to the multiplexer which sequences through the 16 pickup coils and the associated settling time between channels.

For the first 250 measurements and the last 300 measurements the coils were stationary and show that the electronic noise is acceptable, causing a jitter of about .3 degrees in the phase data. However the noise level increased dramatically after the system began moving.

This was the first test conducted with the Russell boards where data was collected while the coils were moving. We believed that the noise was due to mechanical vibrations of the pickup coils interacting with the residual magnetic fields in the pipe itself. Tests with the system designed to be more rigid and pulled smoother verified this conclusion.

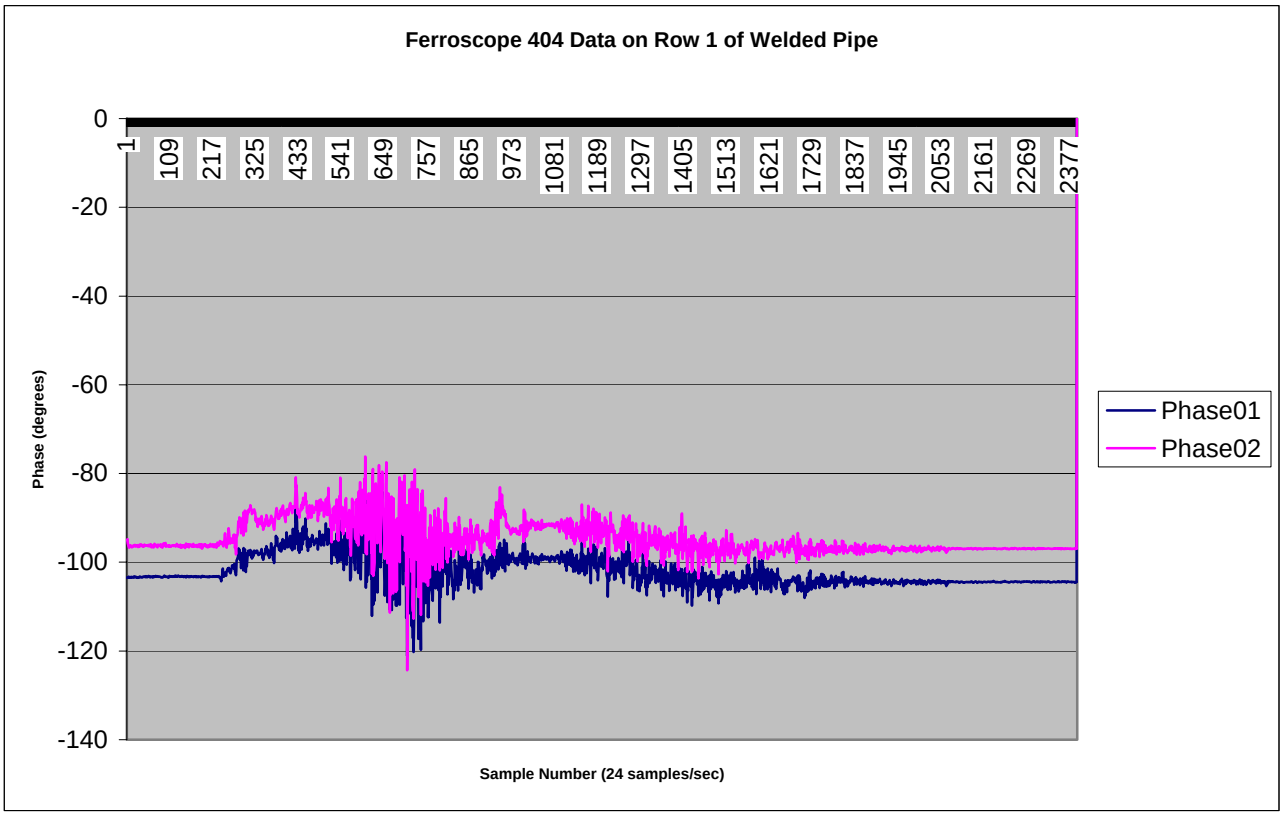

Figure 19: Data from defect line1 using the Russell board.

We rebuilt the part that the two pick-up coils were mounted to by adding wheel supports. The wheel supports enabled a smooth pull through the pipe by reducing the mechanical vibrations of the coils and avoiding any scraping against the pipe wall. Data taken with the rebuilt system is shown in Figure 20. We were able to detect two defects. The sizes of these defects are 1”, 30%wt and ½”, 70%wt.

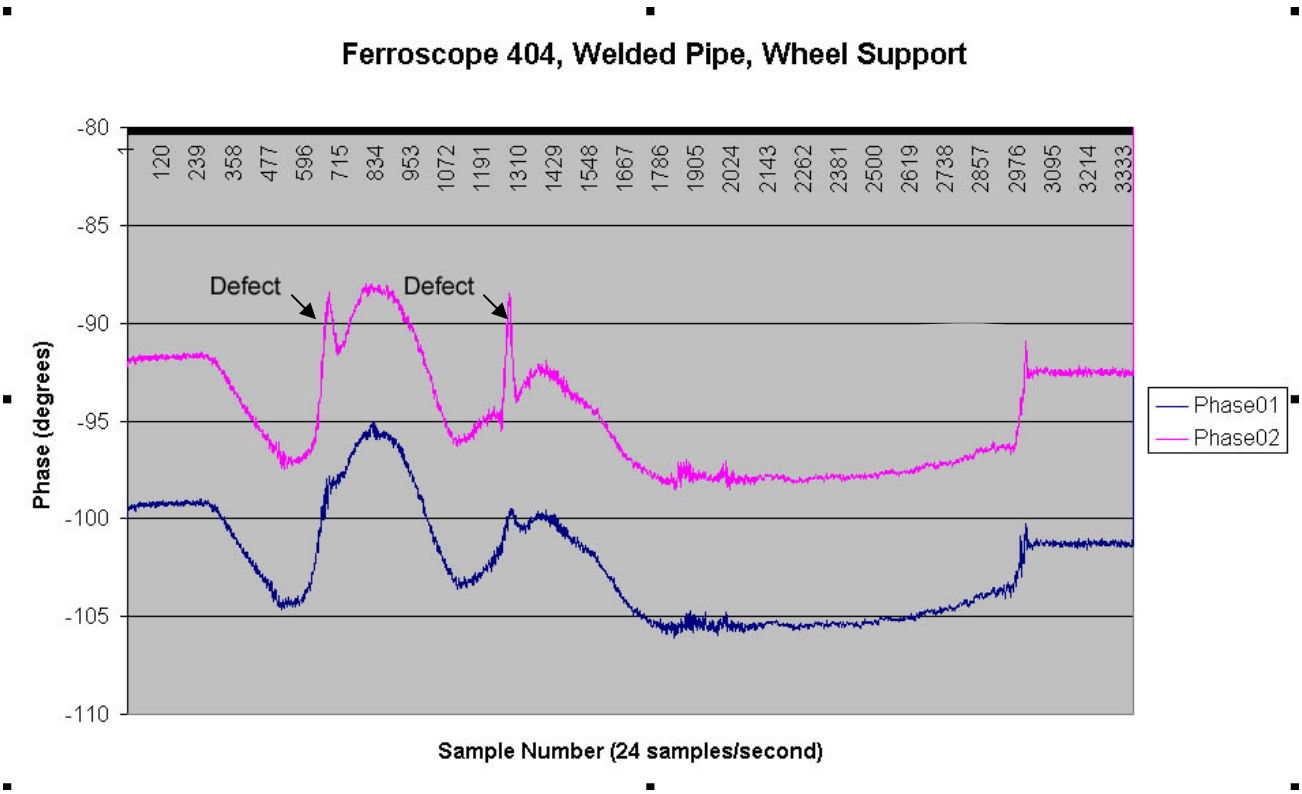

Figure 20: Phase data from defect line one of the seam welded pipe using the Russell boards with wheel supports.

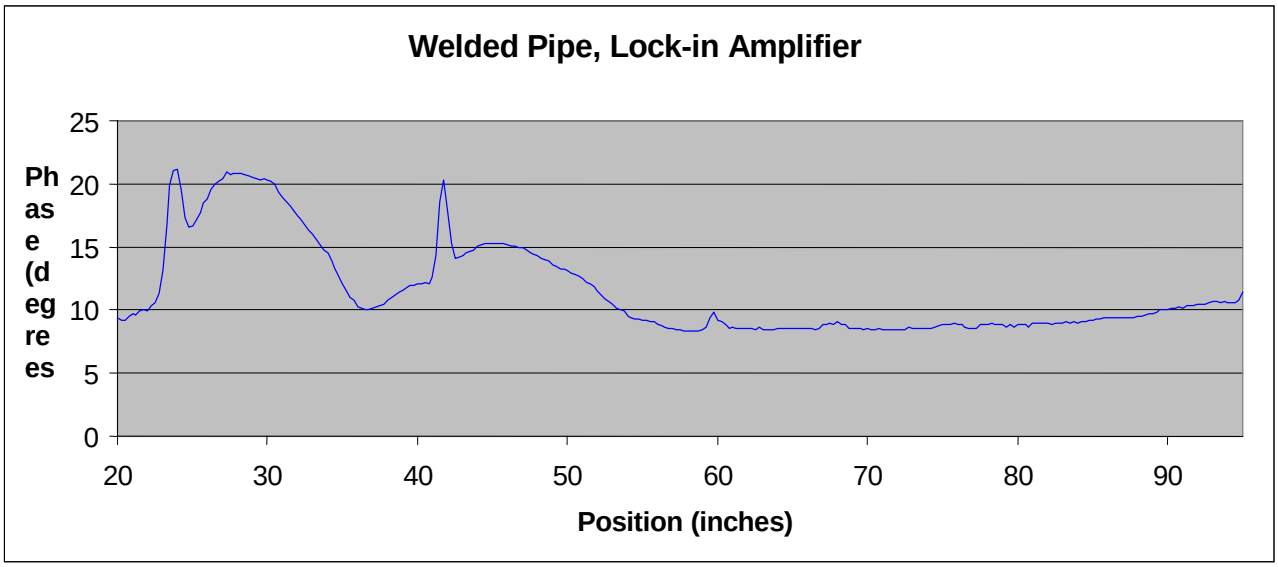

Figure 21: Phase data from defect line one of the seamless pipe using the Lock-in Amplifier.

After inspecting defect line number one using the Russell boards, we noticed that the noise in the data appeared greater than for the lock-in amplifier that we had been using. For comparison purposes, we repeated the inspection using a lock-in amplifier, shown in Figure 21. An rms calculation of noise levels in the phase data gives .21° rms for the Russell Boards and .16° for the Lock-in Amplifier. This normally would indicate that the two are very similar; however, noise from the Russell board comes in bursts. From the lock-in, noise is continuous. The peak burst for the Russell board is 1° peak-to-peak and for the lock-in is .2-.3° peak-to-peak. These differences are the reason that the ½", 30% defect is detected by the lock-in amplifier as shown in Figure 21 but not detected by the Russell board in Figure 20. In actual application this should not be a serious concern since the flaws of interest would be larger that this.

We also conducted tests using the Russell boards while driving the exciter coil with a square wave. The motivation for using a square wave rather than a sine wave is that the square wave drive circuitry requires less power. The tests were performed at various frequencies between 5-95Hz. 25, 65, and 85Hz are shown in the figures below.

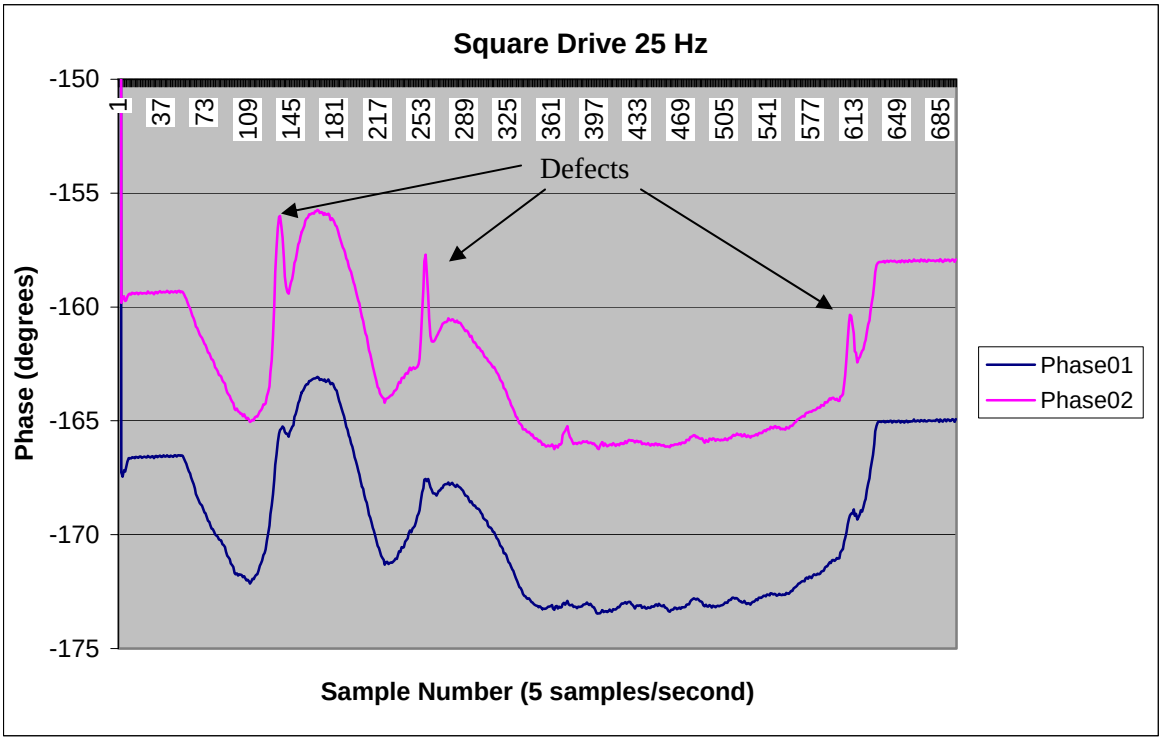

Figure 22: Phase data taken while driving the exciter coil with a 25Hz square wave.

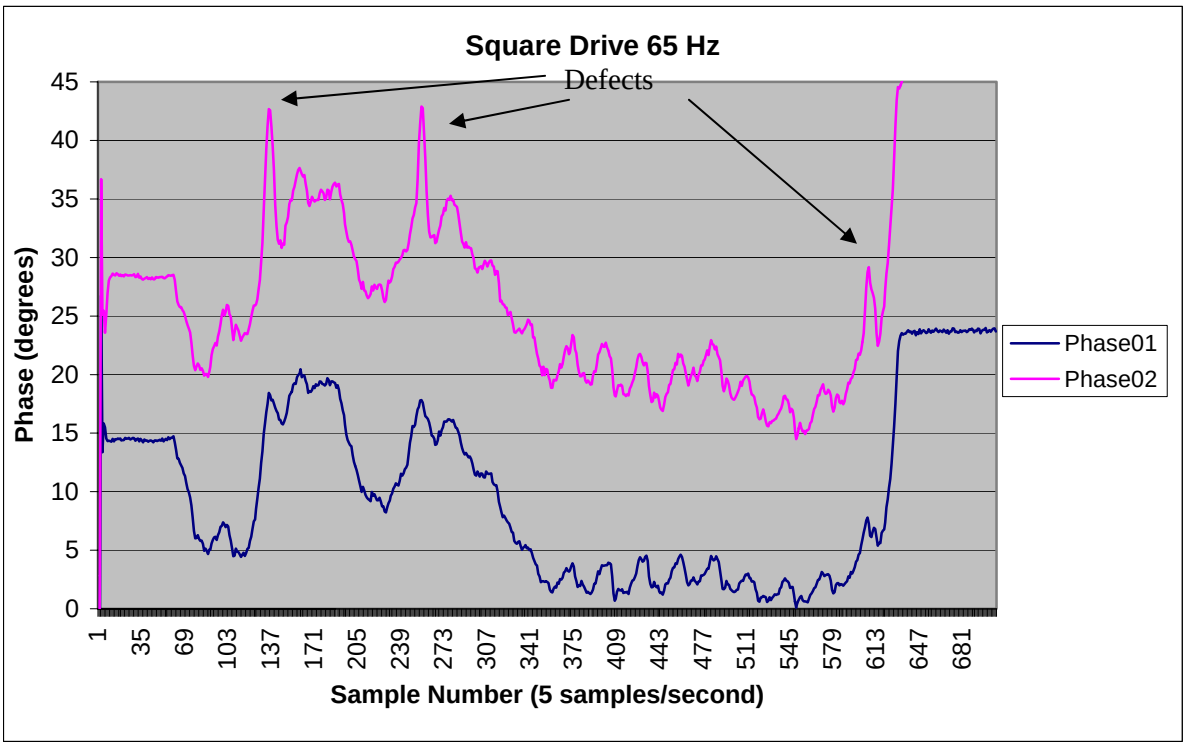

Figure 23: Phase data taken while driving the exciter coil with a 65Hz square wave.

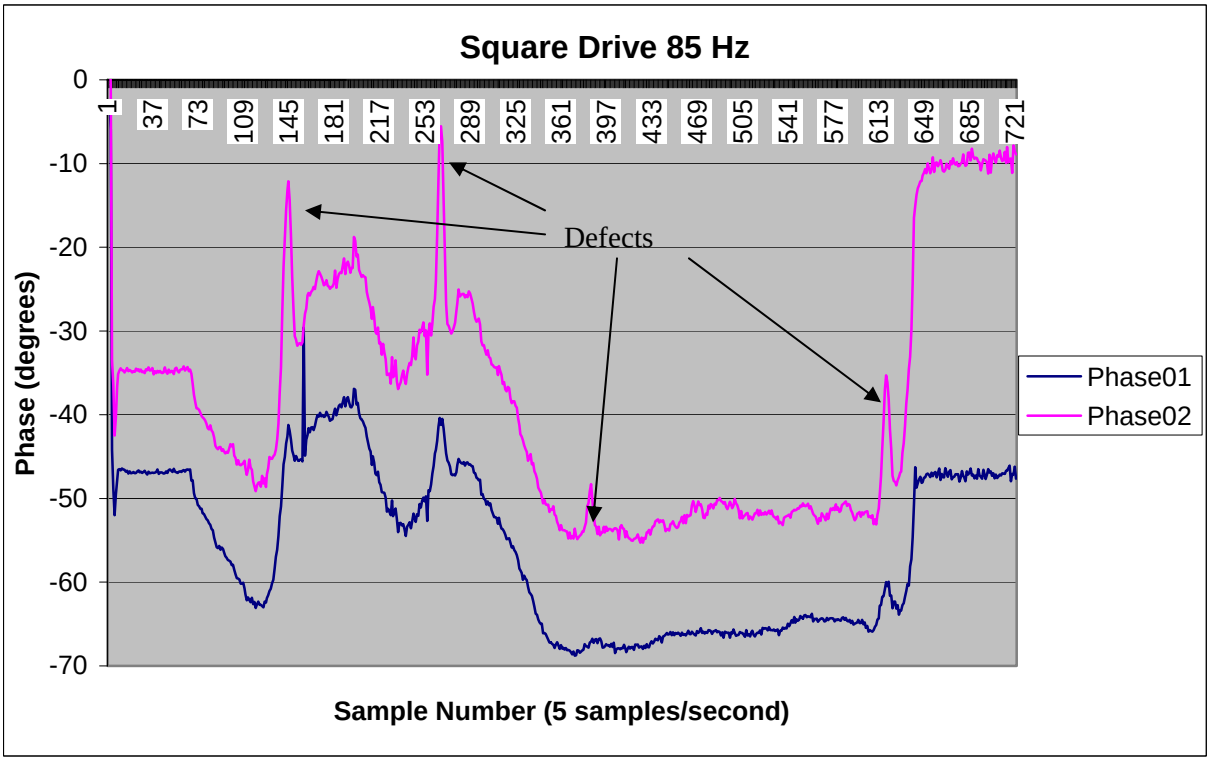

Figure 24: Phase data taken while driving the exciter coil with an 85Hz square wave.

Results of the 25Hz scan, shown in Figure 22, show 4 of 5 defects. Noise levels look reasonable. Starting at 45Hz and up to 75Hz, there was quite a disturbance in the noise. It seems to be periodic and we suspect it may be interference from 60Hz signals created by standard electronic devices (lights, computers, etc.) We only detected 3 of 5 defects during the 65Hz scan, shown in Figure 23, but it is interesting to note that the amplitude of the defect signals is considerably larger, about 3x. The amplitudes of the defect signals in the 85Hz in Figure 24 are 4-5x larger than the signals in the 25Hz test. The periodic type noise is reduced in the 85Hz test and 4 of 5 defects were detected.

We have observed that changes in permeability, the magnetic property of the pipe, affect the amplitude and phase response of the RFEC. To date we rely on the small lengths of the artificial flaws to distinguish between flaws and permeability changes. In Figure 25 below the sharp spikes from coil 2 (Phase02) at 121, 250, 370, and 601 are artificial flaws while the gradual peaks at 161 and 281 are permeability changes caused by pipe magnetization. We realize that real corrosion can be much longer and that it may be more difficult to distinguish between them.

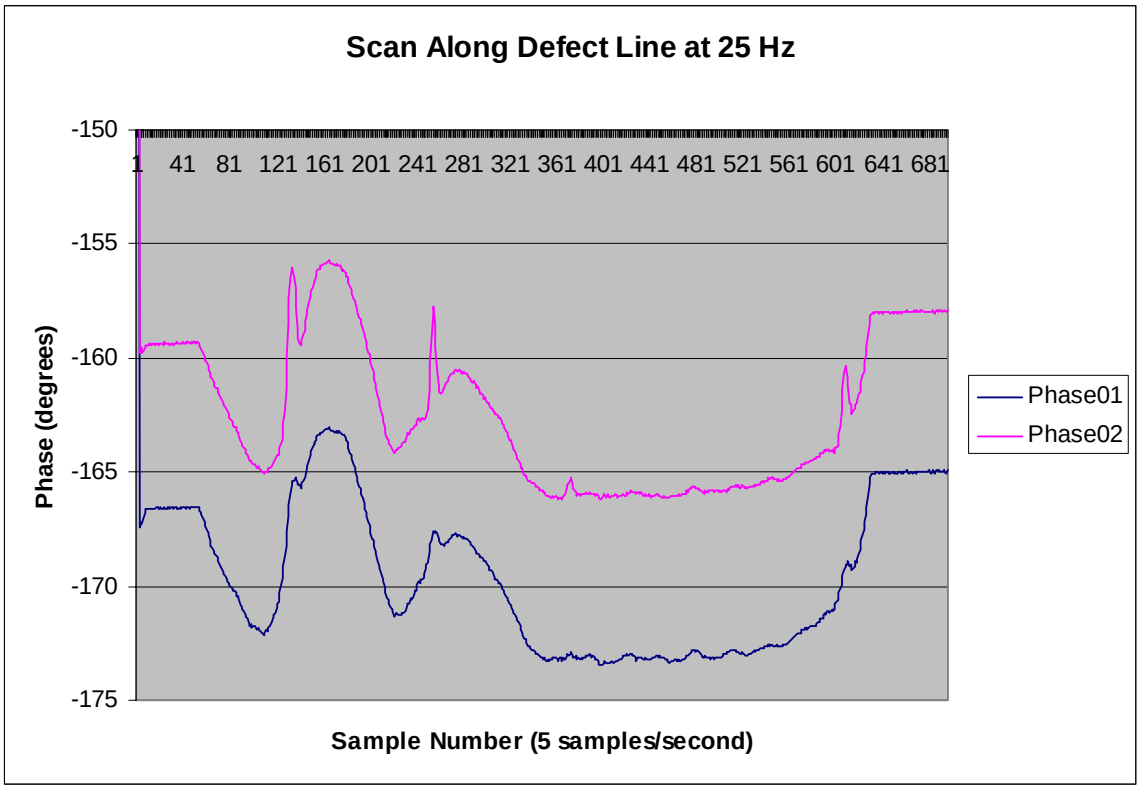

Figure 25: Defect scan at 25Hz

It is possible that analysis at several frequencies may help. The first step was to look at phase information as a function of frequency. The magnitude of the phase deviations at three artificial flaw locations was measured at different frequencies and was found to increase linearly with frequency up to 75 Hz. The results are shown in Figure 26. Flaw one is 1" diameter flat bottom 30% deep, flaw two is ½" diameter round bottom 70% deep and flaw five is 1" diameter round bottom 30% deep. There is a sharp increase at 95 Hz and then there is no detectable flaw signal at higher frequencies. The flaws do show up in the amplitude signal indicating that the analysis should be conducted in the complex plane.

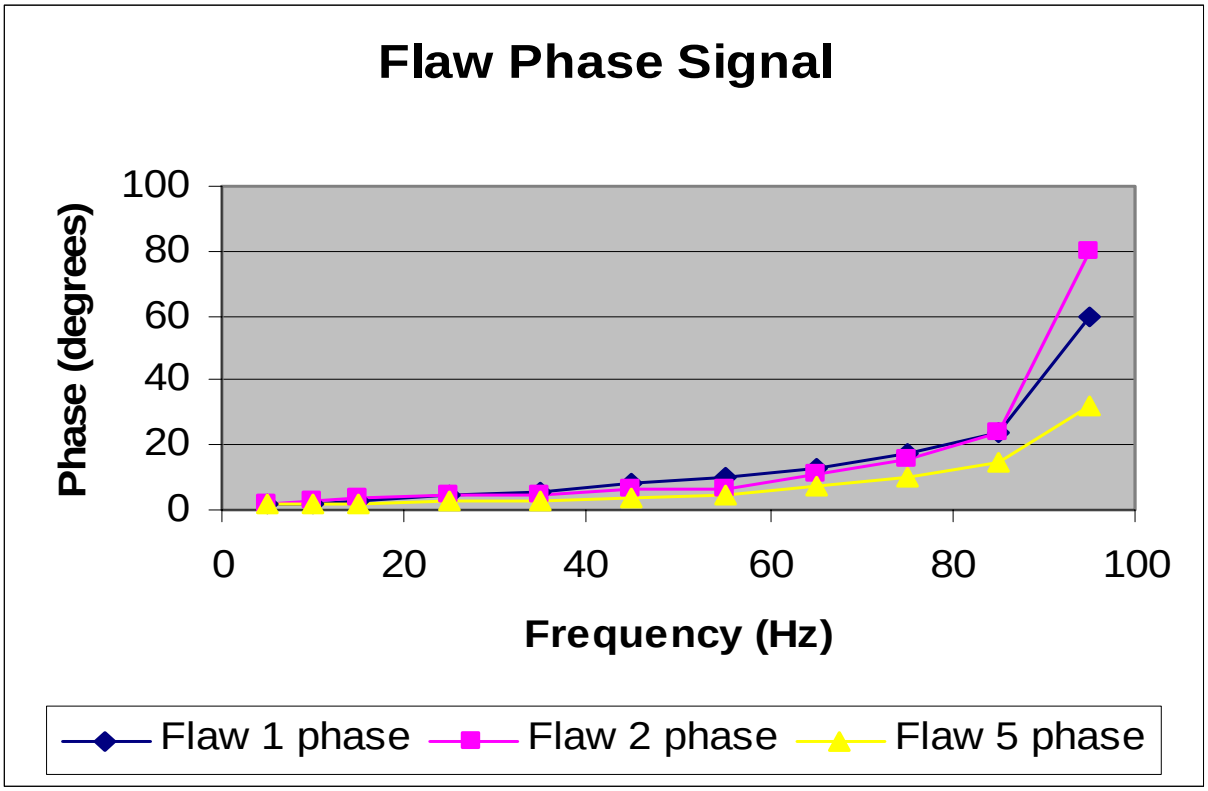

Figure 26: Flaw phase signal

The difference in phase between two locations with different permeability was plotted against frequency and found to also be linear with a sharp increase at 95 Hz. This plot is shown in Figure 27. The similarity of the responses indicates that it may be difficult to distinguish between permeability and gradual thickness changes using phase alone. We expect better results analyzing data in the complex plane. The behavior at higher frequencies is still puzzling and we plan on investigating it in more detail.

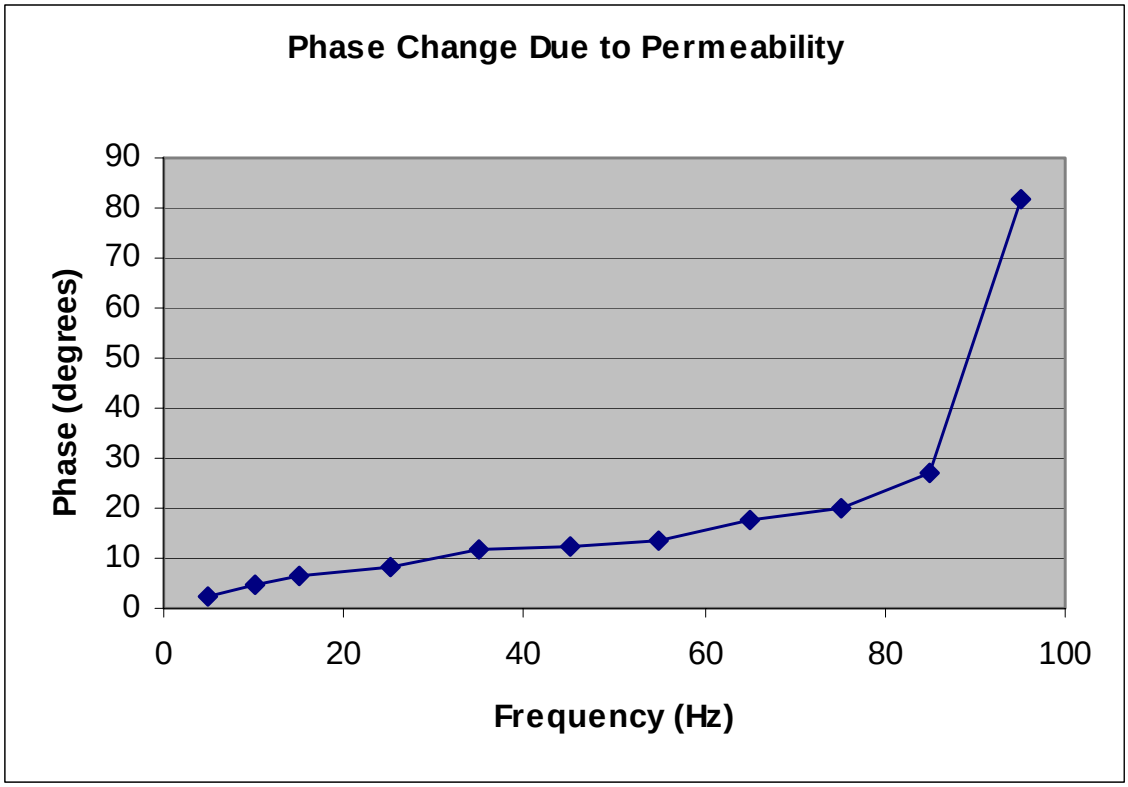

Figure 27: Phase change due to permeability

CONCLUSION

We have accomplished all of our goals and have met all of our deliverables to date. Important points of our accomplishments include optimization of the exciter coil, acquisition of improved detection equipment, and preliminary module designs. All of these are important because they bring us closer to our goal of creating an innovative inspection tool for the natural gas industry. This tool will be capable of inspecting unpiggable pipelines. This sensor integrated Explorer II robot will address the need to inspect unpiggable lines in high consequence areas by one of the four methods mandated by the Pipeline Integrity Management Rule.

Because we have had much success in laboratory work, we remain confident that RFEC will in fact be well suited for use on Explorer II. We have been able to reduce power consumption of the exciter coil to a level compatible with the battery supply on the robot. Through geometric changes and additional modifications, we were able to accomplish reducing the power consumption without compromising detection abilities. The acquisition of the Ferroscope and Adept Pro software from Russell Technologies will prove beneficial to the

project since the Ferroscope can acquire data at the expected speed of travel of Explorer II. Preliminary module design shows that RFEC components are in fact small enough to work on a robotic platform capable of traversing unpiggable pipelines. We expect to be able to fit all of our equipment into the two designated robot modules while still being able to inspect all 360° of the pipe wall.

As a result of the work performed on this project during the first year of the Inspection Technologies program, GTI has proven that the RFEC technology makes an outstanding partner for the Explorer II robotic platform. With continued effort and success, the natural gas industry will have a prototype tool capable of inspecting unpiggable pipelines by the close of this program.

REFERENCES

W.R. McLean, W. R., US Patent 2,573,799, “Apparatus for Magnetically Measuring Thickness of Ferrous Pipe”, Nov. 6, 1951

Schmidt, T. R., “The Casing Instrument Tool-…”, Corrosion, pp 81-85, July 1961

Atherton, D. L., US patent 6,127,823, “Electromagnetic Method for Non-Destructive Testing of Prestressed Concrete Pipes for Broken Prestressed Wires”, Oct. 3, 2000

TABLE OF FIGURES

LIST OF ACRONYMS AND ABBREVIATIONS

RFEC	Remote Field Eddy Current
GTI	Gas Technology Institute
BOP	Bipolar Operational Amplifier
V rms	Volts root mean square
A rms	Amps root mean square
MUX	Multiplexer
mV	Millivolt
W	Watt
UML	Unified Modeling Language
MFL	Magnetic Flux Leakage
DOE	Department of Energy
NETL	National Energy Technology Laboratory
wt	Wall Thickness
Hz	Hertz